mathematics

MDPI

Article

Mathematical Models of the Phase Voltages of High-, Medium- and Low-Voltage Busbars in a Substation during a Phase-to-Ground Fault on High-Voltage Busbars

Dumitru Toader [1,*] and Maria Vintan [2]

[1] Department of Fundamental Physics for Engineers, Politehnica University, 300006 Timisoara, Romania
[2] Department of Computer Sciences and Electrical Engineering, Lucian Blaga University, 550024 Sibiu, Romania; maria.vintan@ulbsibiu.ro
* Correspondence: dumitru.toader@upt.ro; Tel.: +40-(256)-403-398

Abstract: The electrical energy supply of industrial equipment is provided by electrical power stations with high- (HT), medium- (MV) and low-voltage (LV) busbars. Consumers are connected to either MV or LV busbars. In this paper, a real power station was considered, through which the gasoline extraction from the well gas installation is powered. Electric consumers (electric motors) supplied by a MV busbar have active power of 13.54 MW, and those fed by a LV busbar have active power of 6.4 MW. Since electrical consumers operate in explosive environments, the design and operating conditions are more severe than in the case of electrical installations operating in non-explosive environments. The case of a single phase-to-ground fault occurring on the HV transmission lines feeding the power station has been analysed. First, the mathematical models for the calculation of the phase voltages, the dissymmetry and asymmetry coefficients, the reduction coefficient of the plus sequence component, and the effective values of the phase voltages were established. The influence of the source impedance (the equivalent impedance of the HV transmission lines) and of the neutral point configuration of the HV/MV medium-voltage transformer on the calculated quantities was analysed. Then, the results obtained using the established mathematical models were compared with those obtained experimentally by provoking a single-phase-to-ground fault near the HV busbars of the real power station. This study has shown that the de-symmetrisation of the phase voltages of the MV and LV busbars is lower when using the Y/Δ connection for the HV/MV transformer. As a result, it is recommended the Y/Δ connection be used for this transformer, instead of the Y_0/Δ connection.

Keywords: mathematical models; three-phase systems; phase-to-ground fault; phase voltages; protection setting

MSC: 94C05; 94C12

check for updates

Citation: Toader, D.; Vintan, M. Mathematical Models of the Phase Voltages of High-, Medium- and Low-Voltage Busbars in a Substation during a Phase-to-Ground Fault on High-Voltage Busbars. *Mathematics* **2023**, *11*, 3032. https://doi.org/10.3390/math11133032

Academic Editor: Nicu Bizon

Received: 5 June 2023
Revised: 28 June 2023
Accepted: 5 July 2023
Published: 7 July 2023

Copyright: © 2023 by the authors. Licensee MDPI, Basel, Switzerland. This article is an open access article distributed under the terms and conditions of the Creative Commons Attribution (CC BY) license (https://creativecommons.org/licenses/by/4.0/).

1. Introduction

Power stations are an important component of an electricity generation, transmission and distribution system [1–3]. An important category is represented by those supplying very high-power consumers. Such power stations are most frequently used in the oil extraction industry, the chemical industry and the metallurgical industry, and contain high-voltage (HV), medium-voltage (MV) and low-voltage (LV) busbars. One of the important operations that gases are subjected to after their extraction from crude oil and gas wells, is the separation and extraction of gasoline, an operation called *degasolination*. The environment in which electrical installations are used for *degasolination* presents an explosion hazard, which is why the conditions imposed on the design and operation of these installations are much more severe [4] compared to ordinary electrical installations. Starting the large number of electric motors powered at medium or low voltage by a power station used in the oil extraction industry presents a complicated problem. For this

reason, it is desirable to eliminate the risk of unnecessary disconnection of the motors. The MV and LV busbars in the power station are equipped with minimum voltage relays [4]. Those relays must be set accordingly so that a single-phase-to-ground fault on the HV transmission lines that feed the HV busbars in the power station does not lead to the unnecessary disconnection of the motors powered from those busbars. Correct setting of these relays requires knowledge of the values of the phase voltages of the MV and LV busbars during such a fault. The symmetry of the three-phase system of the phase voltages related to the MV and LV busbars is most strongly affected if the single-phase-to-ground fault occurs on the HV busbars in the power station, which is why such a fault was analysed in this paper. Also, most faults that occur in electrical networks are of the single-phase-to-ground type. The authors in [5] stated that these faults represent more than two-thirds of all the short-circuits, and the authors in [6] stated that these faults represent more than 80% of total faults.

The single-phase-to-ground faults that occur at low, medium or high voltages have been analysed in many scientific studies, but the highly diversified structure of electrical installations and the consequences of these faults, from the point of view of supplying electricity to consumers, means this problem continues to be topical.

The authors in [7] analysed the phase-to-ground fault at the LV level using the symmetrical components method. The values of the fault currents were determined in order to choose the fuses necessary for the protection of low-voltage electrical installations. The authors in [8] analysed the phase-to-ground fault that occurring on the 110 kV and 220 kV lines that interconnect electrical substations used in electric traction. The authors in [9–11] analysed the possibilities of limiting the values of the phase-to-ground fault current so as to not exceed the breaking current value of the 500 kV circuit breakers, when the fault occurred on the 500 kV busbar of the electrical substation. The advantages of the symmetrical components method were highlighted, and the results obtained were verified by numerical simulation using the PSCAD (power systems computer-aided design)/EMTDC (electromagnetic transients including DC) software. The authors in [12] analysed a phase-to-ground fault occurring on a 154 kV line by using numerical methods implemented in the MATLAB/Simulink programming environment. The authors in [13] analysed the influence of the transformer connection through which UHVDC (high-voltage direct current) is supplied on the value of the phase-to-ground fault current, at a voltage of 500 kV. It was proposed, in order to limit the value of the fault current, to insert a coil into the neutral part of the transformer. The authors in [14] proposed supplementing the sequence schemes used for the calculation of the phase-to-ground fault current with a non-linear element to reproduce the behaviour of the current limiters (ScFCL—fault current limiters). The results obtained using the model proposed by the authors were compared with those obtained using the EMTDC (electromagnetic transients including DC) software and a good agreement was found. In [15], a mathematical model was presented for the calculation of the phase-to-ground fault current, which combines the method of symmetrical components with the use of phase quantities. It was highlighted that the use of the symmetrical components method greatly simplifies the calculation of the phase-to-ground fault current. The authors in [5] highlighted the difficulty of performing measurements in electrical IT installations, which is why analytical mathematical models are used in the study of faults, and the obtained results are verified using numerical models.

The operation of electrical consumers has been shown to be affected by the change in their supply voltage value [16]. The authors in [17] investigated the factors that influence financial losses due to a decrease in the value of the supply voltage of the equipment used in industrial processes. In [18,19], the sensitivity curves of industrial equipment were determined, and a series of international standards were established that provide guidelines in the design of equipment to increase the ability to pass through voltage drops, such as the curves of tolerance recommended in IEEE 1346 [20]. In the IEEE 1564 standard, ITIC and SEMI F47 reference curves are recommended to calculate the severity of voltage reductions [21]. In the absence of precise criteria regarding the behaviour

of electrical equipment during voltage sags, it is recommended to use the ITIC and SEMI standards [22–24].

This study completes the specialized literature by presenting the mathematical models used to calculate the phase voltages of the HV, MV and LV busbars of a real power station, in the event of a single-phase-to-ground fault on the HV transmission lines. Furthermore, it presents a comparison with the experimental results of a single-phase-to-ground fault intentionally initiated near the HV busbars of a real power station. A single-phase-to-ground fault in HV electrical installations can lead to serious consequences, which is why such an experiment is very difficult to perform. For this reason, few experimental results obtained in real installations have been presented in the literature. It is important and useful to provide researchers with the results of measurements carried out in a real power station under analysis.

2. Objectives and the Studied Case

The single-line diagram of the real power station included in this study, through which the gasoline extraction from the well gas installation (the *degasolination* installation) is powered, is shown in Figure 1. The power station has three voltage levels: high, medium and low. The line voltages for the three levels are 110 kV, 6 kV and 0.4 kV.

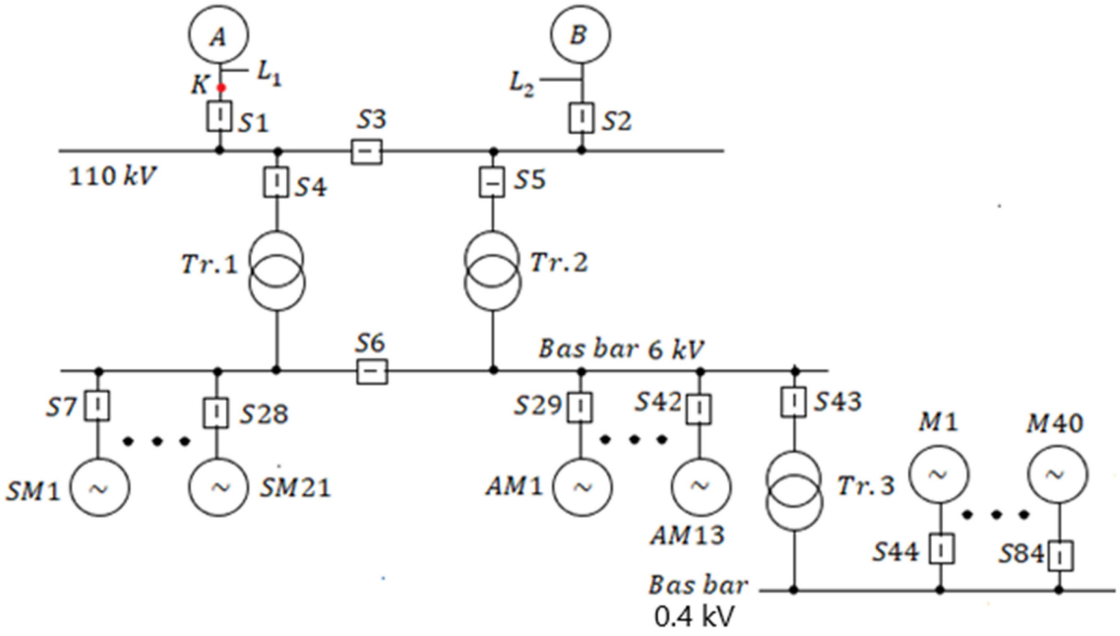

Figure 1. Single-line diagram of the transformation station related to the degasolination plant.

The notations in Figure 1 have the following meanings: S1–S5, switches with nominal voltage 110 kV; S6–S43, switches with nominal voltage 6 kV; S44–S84, switches with nominal voltage 0.4 kV; L1 and L2, 110 kV power lines; A, the 220/110 kV transformer station from which the L1 line is fed; B, the 220/110 kV transformer station from which the L2 line is fed; SM1–SM21, synchronous motors with nominal voltage of 6 kV; AM1–AM13, asynchronous motors with nominal voltage of 6 kV; Tr.1 and Tr.2, 110/6 kV transformers; Tr.3, transformer 6/0.4 kV; M1–M40, asynchronous motors with nominal voltage of 0.4 kV.

Considering a single-phase-to-ground fault that occurs on one of the 110 kV transmission lines that feed the power station, the contribution of this paper can be considered as:

(1) Establishing the mathematical models for the calculation of the phase voltages related to the 110 kV, 6 kV and 0.4 kV busbars, and for the calculation of the fault current.
(2) Establishing the mathematical models for the dissymmetry coefficient and asymmetry coefficient, related to the three-phase voltages of the 110 kV, 6 kV and 0.4 kV busbars.

(3) Experimental determination of the phase voltages related to the 110 kV, 6 kV and 0.4 kV busbars, and of the fault current.
(4) Establishing the way in which the power station must be supplied, and the neutral point configuration of the 110 kV/6 kV transformer, so that the value of the dissymmetry coefficient has the minimum values.
(5) Determination of the reduction coefficient of the plus sequence component of the phase voltages related to the 110 kV, 6 kV and 0.4 kV busbars.

From the 6 kV busbars of the analysed power station, 21 synchronous motors and 13 asynchronous motors are fed, and from the 0.4 kV busbars, 40 asynchronous motors are fed. A phase-to-ground fault occurring in an electrical network causes the three-phase system of phase voltages to become unbalanced. The degree of asymmetry in the three-phase system of the phase voltages is characterized by the dissymmetry coefficient (k^-) and by the asymmetry coefficient (k^0). For synchronous and asynchronous electric motors, the negative sequence component determines a torque in the opposite direction to that created by the plus sequence component, i.e., it generates a braking torque.

Due to a single-phase-to-ground fault produced on the 110 kV transmission lines, the disconnection from the source of the motors fed from the 6 kV busbars and of those fed from the 0.4 kV busbars leads to the *degasolination* installations being taken out of operation for a relatively long period of time. The time required to start these motors (if one considers only two minutes being required to start a motor) is 2 h and 28 min. During this time, the *degasolination* operation can no longer be carried out, which leads to significant financial losses for the company concerned. It is therefore important to use a consumer supply scheme that leads to a lower de-symmetrisation of the phase voltages related to the 6 kV and 0.4 kV busbars, and during a phase-to-ground fault occurring on the 110 kV lines feeding the 110 kV busbars of the power station.

This study analysed the quantities that influence the change in the phase voltages of the HV, MV and LV busbars, the dissymmetry and asymmetry coefficients, and the reduction ratio of the plus sequence component during a single-phase-to-ground fault that occurs near the HV busbars of the power station (point *K* in Figure 1).

The 110 kV busbar of the power station can be fed by one or two of the 110 kV transmission lines. The following cases were analysed:

(A) Fed by two 110 kV lines and the transformer Tr.1 has the connection Y_0/Δ.
(B) Fed by two 110 kV lines and the transformer Tr.1 has the Y/Δ connection.
(C) Fed by one 110 kV line L_1 and the transformer Tr.1 has the Y_0/Δ connection.
(D) Fed by the 110 kV line L_1 and the transformer Tr.1 has the Y/Δ connection.

In all cases, it was considered that the transformer Tr.2 was disconnected from the 110 kV busbar.

For cases (C) and (D), the results obtained using the established mathematical models were verified experimentally.

3. Materials and Methods (Mathematical Models)

Information flow diagram for determining the mathematical models of the phase voltages related to the HV, MV and LV bars of the substation, the dissymmetry and asymmetry coefficients related to the HV, MV, LV bars, and the reduction coefficient of the plus sequence component during the phase-ground fault, at point K in Figure 1, are shown in Figure 2.

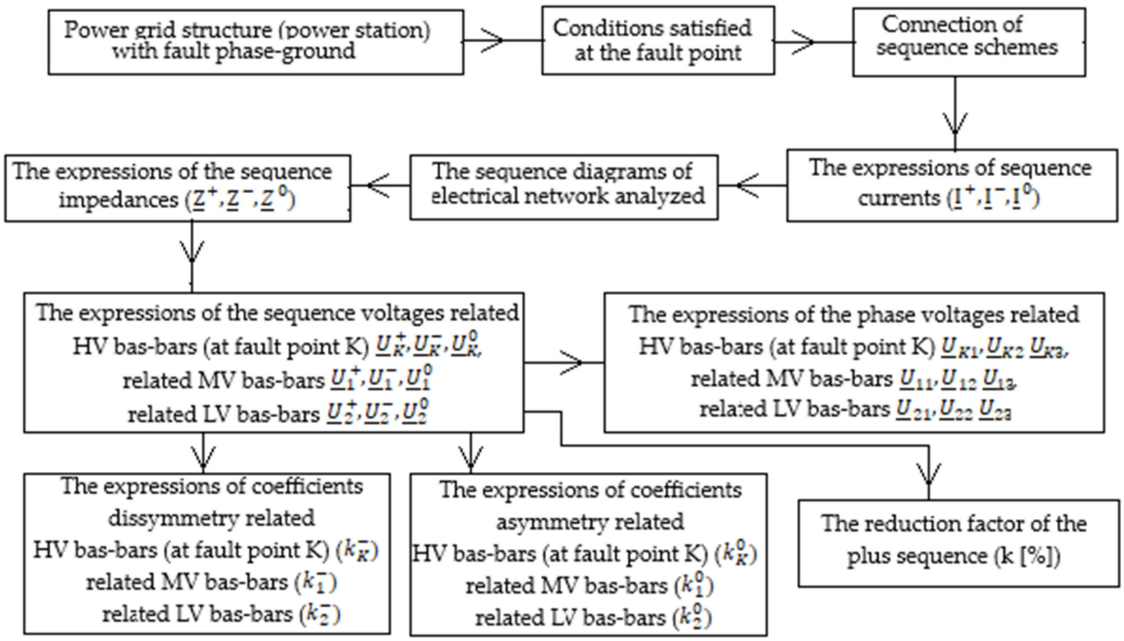

Figure 2. Information flow diagram for establishing mathematical models of phase voltages, coefficients of dissymmetry, asymmetry and plus sequence voltage reduction.

Establishing the mathematical models for determining the phase voltages related to the HV, MV, and LV busbars of the power station, using the sequence components method, involved the following steps:

Step 1: Establishing the method of connecting the sequence schemes for a single-phase-to-ground fault.
Step 2: Setting up the mathematical model for calculating the sequence currents.
Step 3: Drawing up the sequence diagrams for the analysed electrical network.
Step 4: Determining the expressions of the sequence impedances related to the analysed network.
Step 5: Determining the sequence voltages corresponding to the HV, MV and LV busbars.
Step 6: Determining the phase voltages related to the HV, MV and LV busbars.
Step 7: Determining the dissymmetry and asymmetry coefficients for the phase voltages of the HV, MV, and LV busbars.
Step 8: Determining the phase voltages as a function of the plus sequence voltage and the coefficients of dissymmetry and asymmetry.
Step 9: Defining the reduction coefficient of the plus sequence component during the single-phase-to-ground fault.

In the literature [6,8–11,13,14,25–28], it has been shown that, in the case of a single-phase-to-ground fault, given the conditions imposed at the fault site, the sequence diagrams are connected in series. From the conditions imposed at the fault site, it follows that the sequence components of the currents at the fault site satisfy Equation (1).

$$\underline{I}^+ = \underline{I}^- = \underline{I}^0 \tag{1}$$

The equivalent sequence diagram of the medium-voltage network in which the single-phase-to-ground fault occurs is shown in Figure 3.

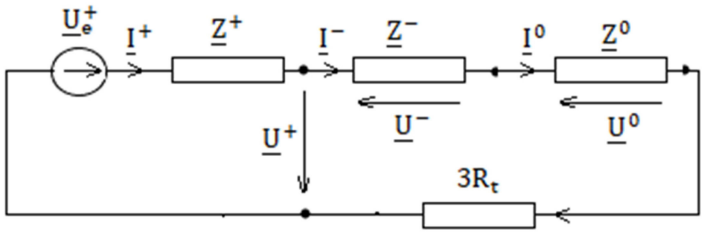

Figure 3. Connection of sequence diagrams in case of a phase-to-ground fault (the figure was revised).

In the diagram in Figure 3, the meanings of the notations are as follows: $\underline{U}_e^+$ represents the plus sequence component of the three-phase voltage system at the fault location in the absence of the fault; $\underline{Z}^+$, $\underline{Z}^-$ and $\underline{Z}^0$ represent the plus, minus and zero-sequence impedances seen from the fault location, in the absence of the fault.

In the literature, it has been accepted (in most cases) that the three-phase system of voltages at the fault site in the absence of the fault is symmetrical [6,8–11,13,25–28]. Therefore, the plus sequence component of the three-phase system of voltage is equal to the phase voltage ($\underline{U}_e^+ = \underline{U}_{ph}$). For fault analysis, the voltage of the phase on which the single-phase-to-ground fault occurs is considered as the reference. As a result, the next relationship is satisfied:

$$\underline{\mathrm{U}}_{\mathrm{e}}^{+} = \underline{\mathrm{U}}_{\mathrm{ph}} = \mathrm{U}_{\mathrm{ph}} \tag{2}$$

From the diagram shown in Figure 3, the expressions for the sequence currents yields are as follows:

$$\underline{\mathrm{I}}^{+} = \underline{\mathrm{I}}^{-} = \underline{\mathrm{I}}^{0} = \frac{\underline{\mathrm{U}}_{\mathrm{e}}^{+}}{\underline{Z}^{+} + \underline{Z}^{-} + \underline{Z}^{0} + 3 * R_t} = \frac{\mathrm{U}_{\mathrm{ph}}}{\underline{Z}^{+} + \underline{Z}^{-} + \underline{Z}^{0} + 3 * R_t} \tag{3}$$

For the calculation of the sequence impedances, the sequence diagrams of the electrical network with the structure shown in Figure 1 were made. The sequence diagrams are shown in Figure 4. The reference level for the voltage was considered to be 110 kV.

The notations in Figure 4 have the following meanings: $\underline{\mathrm{U}}_{\mathrm{ph}}$—the phase voltage at the fault location before the fault occurs (point K); $\underline{\mathrm{U}}_{\mathrm{K}}^{+}, \underline{\mathrm{U}}_{\mathrm{K}}^{-}, \underline{\mathrm{U}}_{\mathrm{K}}^{0}$—the sequence components of the voltages at the fault location (110 kV); $\underline{\mathrm{U}}_{1}^{+}, \underline{\mathrm{U}}_{1}^{-}, \underline{\mathrm{U}}_{1}^{0}$—the sequence components of the voltages related to the medium-voltage busbars (6 kV); $\underline{\mathrm{U}}_{2}^{+}, \underline{\mathrm{U}}_{2}^{-}, \underline{\mathrm{U}}_{2}^{0}$—the sequence components of the voltages related to the low-voltage busbars (0.4 kV); $\underline{\mathrm{Z}}_{1}^{+}, \underline{\mathrm{Z}}_{1}^{-}, \underline{\mathrm{Z}}_{1}^{0}$—sequence impedances of line L_1 from Figure 1; $\underline{\mathrm{Z}}_{2}^{+}, \underline{\mathrm{Z}}_{2}^{-}, \underline{\mathrm{Z}}_{2}^{0}$—sequence impedances of line L_2 from Figure 1; $\underline{\mathrm{Z}}_{\mathrm{Tr1}}^{+}, \underline{\mathrm{Z}}_{\mathrm{Tr1}}^{-}, \underline{\mathrm{Z}}_{\mathrm{Tr1}}^{0}$—sequence impedances of the 110/6 kV transformer marked Tr.1 in Figure 1; $\underline{\mathrm{Z}}_{\mathrm{Tr3}}^{+}, \underline{\mathrm{Z}}_{\mathrm{Tr3}}^{-}, \underline{\mathrm{Z}}_{\mathrm{Tr3}}^{0}$—sequence impedances of the 6/0.4 kV transformer marked Tr.3 in Figure 1; $\underline{\mathrm{Z}}_{\mathrm{c1}}^{+}, \underline{\mathrm{Z}}_{\mathrm{c1}}^{-}, \underline{\mathrm{Z}}_{\mathrm{c1}}^{0}$—sequence impedances of the consumers fed from the medium-voltage busbars (6 kV busbar in Figure 1) of the power station (synchronous motors and asynchronous motors); $\underline{\mathrm{Z}}_{\mathrm{c2}}^{+}, \underline{\mathrm{Z}}_{\mathrm{c2}}^{-}, \underline{\mathrm{Z}}_{\mathrm{c2}}^{0}$—sequence impedances of the consumers fed from the low-voltage busbars (0.4 kV busbar in Figure 1) of the power station (asynchronous motors and auxiliary services); and R_t—resistance through the fault location.

For the calculation of the plus, minus and zero-sequence impedances, the diagrams from Figure 4a–c were used. According to the equivalent voltage generator theorem (Thévenin's theorem), the internal impedance of the equivalent voltage generator is equal to the equivalent impedance of the passivated circuit, as seen from the fault location, in the absence of the fault. In Figure 4a–c, the fault location is denoted by K. As a result, the sequence impedances are the equivalent impedances seen from point K, and the null, points between which the sequence voltages are represented.

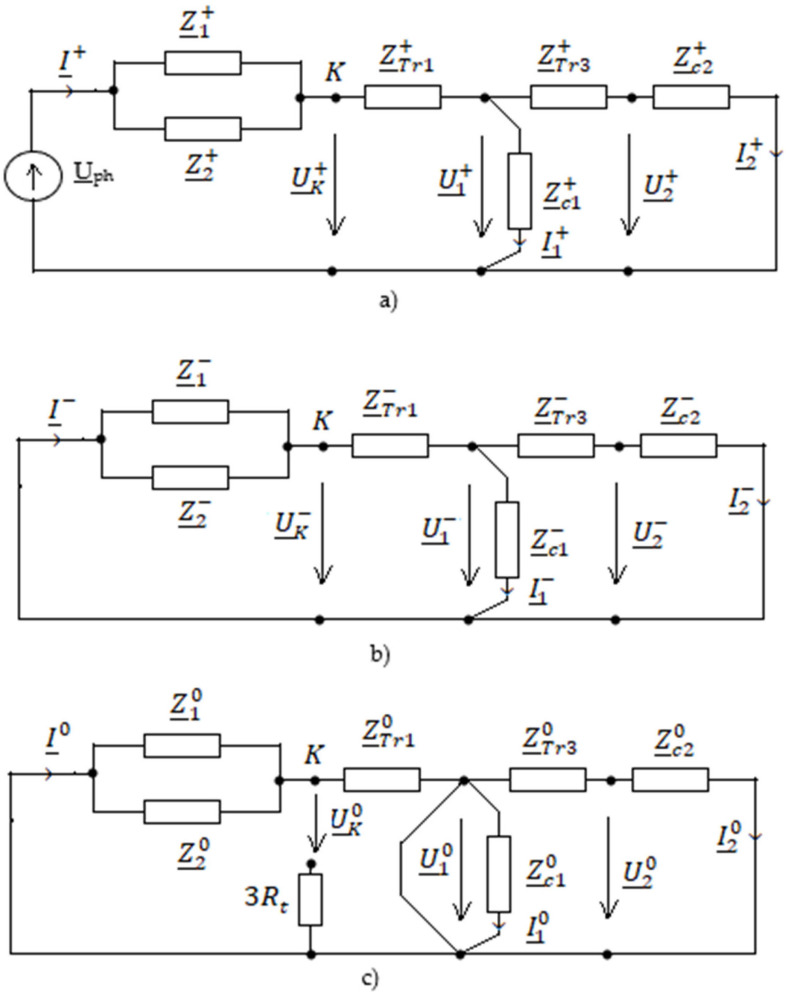

Figure 4. Sequence diagrams. (**a**) The positive sequence. (**b**) The negative sequence. (**c**) Sequence zero.

Considering the sequence diagrams (Figure 4), for the sequence impedances seen from the fault location (point K in Figure 4), the next expressions are obtained:

$$\underline{Z}^{+} = \frac{\frac{\underline{Z}_1^{+} * \underline{Z}_2^{+}}{\underline{Z}_1^{+} + \underline{Z}_2^{+}} * \left(\underline{Z}_{\mathrm{Tr1}}^{+} + \frac{\underline{Z}_{\mathrm{c1}}^{+} * \left(\underline{Z}_{\mathrm{c2}}^{+} + \underline{Z}_{\mathrm{Tr3}}^{+} \right)}{\underline{Z}_{\mathrm{c1}}^{+} + \underline{Z}_{\mathrm{c2}}^{+} + \underline{Z}_{\mathrm{Tr3}}^{+}} \right)}{\frac{\underline{Z}_1^{+} * \underline{Z}_2^{+}}{\underline{Z}_1^{+} + \underline{Z}_2^{+}} + \underline{Z}_{\mathrm{Tr1}}^{+} + \frac{\underline{Z}_{\mathrm{c1}}^{+} * \left(\underline{Z}_{\mathrm{c2}}^{+} + \underline{Z}_{\mathrm{Tr3}}^{+} \right)}{\underline{Z}_{\mathrm{c1}}^{+} + \underline{Z}_{\mathrm{c2}}^{+} + \underline{Z}_{\mathrm{Tr3}}^{+}}} \tag{4}$$

$$\underline{Z}^{-} = \frac{\frac{\underline{Z}_1^{-} * \underline{Z}_2^{-}}{\underline{Z}_1^{-} + \underline{Z}_2^{-}} * \left(\underline{Z}_{\mathrm{Tr1}}^{-} + \frac{\underline{Z}_{\mathrm{c1}}^{-} * \left(\underline{Z}_{\mathrm{c2}}^{-} + \underline{Z}_{\mathrm{Tr3}}^{-} \right)}{\underline{Z}_{\mathrm{c1}}^{-} + \underline{Z}_{\mathrm{c2}}^{-} + \underline{Z}_{\mathrm{Tr3}}^{-}} \right)}{\frac{\underline{Z}_1^{-} * \underline{Z}_2^{-}}{\underline{Z}_1^{-} + \underline{Z}_2^{-}} + \underline{Z}_{\mathrm{Tr1}}^{-} + \frac{\underline{Z}_{\mathrm{c1}}^{-} * \left(\underline{Z}_{\mathrm{c2}}^{-} + \underline{Z}_{\mathrm{Tr3}}^{-} \right)}{\underline{Z}_{\mathrm{c1}}^{-} + \underline{Z}_{\mathrm{c2}}^{-} + \underline{Z}_{\mathrm{Tr3}}^{-}}} \tag{5}$$

$$\underline{Z}^{0} = \frac{\frac{\underline{Z}_1^{0} * \underline{Z}_2^{0}}{\underline{Z}_1^{0} + \underline{Z}_2^{0}} * \underline{Z}_{\mathrm{Tr1}}^{0}}{\frac{\underline{Z}_1^{0} * \underline{Z}_2^{0}}{\underline{Z}_1^{0} + \underline{Z}_2^{0}} + \underline{Z}_{\mathrm{Tr1}}^{0}} \tag{6}$$

The sequence voltages related to the high-voltage busbar (110 kV in Figure 1 and denoted by $\underline{U}_{\mathrm{K}}^{+}, \underline{U}_{\mathrm{K}}^{-}, \underline{U}_{\mathrm{K}}^{0}$ in Figure 4) are given by the following expressions:

$$\underline{U}_{\mathrm{K}}^{+} = \underline{U}_{\mathrm{ph}} - \underline{Z}^{+} * \underline{I}^{+} \tag{7}$$

$$\underline{U}_{\mathrm{K}}^{-} = -\underline{Z}^{-} * \underline{I}^{-} \tag{8}$$

$$\underline{U}_K^0 = -\underline{Z}^0 * \underline{I}^0 \tag{9}$$

The sequence voltages related to the medium-voltage busbar (6 kV in Figure 1 and denoted $\underline{U}_1^+, \underline{U}_1^-, \underline{U}_1^0$ in Figure 4) are given by the following expressions:

$$\underline{U}_K^+ = \underline{U}_1^+ = \underline{U}_K^+ * \left(1 - \frac{\underline{Z}_{Tr1}^+}{\underline{Z}_{Tr1}^+ + \frac{\underline{Z}_{c1}^+ \left(\underline{Z}_{Tr3}^+ + \underline{Z}_{c2}^+\right)}{\underline{Z}_{c1}^+ + \underline{Z}_{Tr3}^+ + \underline{Z}_{c2}^+}}\right) \tag{10}$$

$$\underline{U}_1^- = \underline{U}_K^- * \left(1 - \frac{\underline{Z}_{Tr1}^-}{\underline{Z}_{Tr1}^- + \frac{\underline{Z}_{c1}^- \left(\underline{Z}_{Tr3}^- + \underline{Z}_{c2}^-\right)}{\underline{Z}_{c1}^- + \underline{Z}_{Tr3}^- + \underline{Z}_{c2}^-}}\right) \tag{11}$$

$$\underline{U}_1^0 = 0 \tag{12}$$

The sequence voltages related to the low-voltage busbar (0.4 kV in Figure 1 and denoted $\underline{U}_2^+, \underline{U}_2^-, \underline{U}_2^0$ in Figure 4) are given by the following expressions:

$$\underline{U}_2^+ = \underline{Z}_{c2}^+ * \underline{I}_2^+ = \frac{\underline{Z}_{c2}^+}{\underline{Z}_{c2}^+ + \underline{Z}_{Tr3}^+} * \underline{U}_1^+ \tag{13}$$

$$\underline{U}_2^- = \underline{Z}_{c2}^- * \underline{I}_2^- = \frac{\underline{Z}_{c2}^-}{\underline{Z}_{c2}^- + \underline{Z}_{Tr3}^-} * \underline{U}_1^- \tag{14}$$

$$\underline{U}_2^0 = 0 \tag{15}$$

Knowing the sequence components of the phase voltages at the fault location, the sequence components of the voltage of the medium- and low-voltage busbars can be determined. The transformation ratio of transformer Tr.1 is k_{Tr1} = 110/6 and of transformer Tr.3 is k_{Tr3} = 6/0.4 (Figure 1).

The phase voltages at the fault location (related to the 110 kV busbars) are expressed as a function of the sequence components through the following relationships:

$$\underline{U}_{K1} = \underline{U}_K^+ + \underline{U}_K^- + \underline{U}_K^0 \tag{16}$$

$$\underline{U}_{K2} = \underline{a}^2 * \underline{U}_K^+ + \underline{a} * \underline{U}_K^- + \underline{U}_K^0 \tag{17}$$

$$\underline{U}_{K3} = \underline{a} * \underline{U}_K^+ + \underline{a}^2 * \underline{U}_K^- + \underline{U}_K^0 \tag{18}$$

The phase voltages related to the medium-voltage busbars are expressed as a function of the sequence components through the following relationships:

$$\underline{U}_{11} = \frac{\underline{U}_1^+ + \underline{U}_1^- + \underline{U}_1^0}{k_{Tr1}} \tag{19}$$

$$\underline{U}_{12} = \frac{\underline{a}^2 * \underline{U}_1^+ + \underline{a} * \underline{U}_1^- + \underline{U}_1^0}{k_{Tr1}} \tag{20}$$

$$\underline{U}_{13} = \frac{\underline{a} * \underline{U}_1^+ + \underline{a}^2 * \underline{U}_1^- + \underline{U}_1^0}{k_{Tr1}} \tag{21}$$

The phase voltages related to the low-voltage busbars are expressed as a function of the sequence components through the following relationship:

$$\underline{U}_{21} = \frac{\underline{U}_2^+ + \underline{U}_2^- + \underline{U}_2^0}{k_{Tr3}} \tag{22}$$

$$\underline{U}_{22} = \frac{\underline{a}^2 * \underline{U}_2^+ + \underline{a} * \underline{U}_2^- + \underline{U}_2^0}{k_{Tr3}} \tag{23}$$

$$\underline{U}_{23} = \frac{\underline{a} * \underline{U}_2^+ + \underline{a}^2 * \underline{U}_2^- + \underline{U}_2^0}{k_{Tr3}} \tag{24}$$

The dissymmetry coefficient is defined as the ratio between the negative and the positive sequence component and is expressed in %. It is calculated using the following expression:

$$\underline{k}^-\% = \frac{\underline{U}^-}{\underline{U}^+} * 100 \tag{25}$$

Considering Equations (3), (7) and (8) for the dissymmetry coefficient at the fault location K (110 kV busbars), the next expression is obtained:

$$\underline{k}_K^- = \frac{\underline{Z}^-}{\underline{Z}^- + \underline{Z}^0 + 3 * R_t} \tag{26}$$

The asymmetry coefficient of the phase voltages related to the medium-voltage busbars (6 kV) in the power station is expressed by the next expression:

$$\underline{k}_1^- = \frac{1 - \frac{\underline{Z}_{Tr1}^-}{\underline{Z}_{Tr1}^- + \frac{\underline{Z}_{c1}^- \left(\underline{Z}_{Tr3}^- + \underline{Z}_{c2}^-\right)}{\underline{Z}_{c1}^- + \underline{Z}_{Tr3}^- + \underline{Z}_{c2}^-}}}{1 - \frac{\underline{Z}_{Tr1}^+}{\underline{Z}_{Tr1}^+ + \frac{\underline{Z}_{c1}^+ \left(\underline{Z}_{Tr3}^+ + \underline{Z}_{c2}^+\right)}{\underline{Z}_{c1}^+ + \underline{Z}_{Tr3}^+ + \underline{Z}_{c2}^+}}} * \underline{k}_K^- \tag{27}$$

The dissymmetry coefficient of the phase voltages related to the low-voltage busbars (0.4 kV) in the power station is given by the next expression:

$$\underline{k}_2^- = \frac{\frac{\underline{Z}_{c2}^-}{\underline{Z}_{c2}^- + \underline{Z}_{Tr3}^-}}{\frac{\underline{Z}_{c2}^+}{\underline{Z}_{c2}^+ + \underline{Z}_{Tr3}^+}} * \frac{1 - \frac{\underline{Z}_{Tr1}^-}{\underline{Z}_{Tr1}^- + \frac{\underline{Z}_{c1}^- \left(\underline{Z}_{Tr3}^- + \underline{Z}_{c2}^-\right)}{\underline{Z}_{c1}^- + \underline{Z}_{Tr3}^- + \underline{Z}_{c2}^-}}}{1 - \frac{\underline{Z}_{Tr1}^+}{\underline{Z}_{Tr1}^+ + \frac{\underline{Z}_{c1}^+ \left(\underline{Z}_{Tr3}^+ + \underline{Z}_{c2}^+\right)}{\underline{Z}_{c1}^+ + \underline{Z}_{Tr3}^+ + \underline{Z}_{c2}^+}}} * \underline{k}_K^- \tag{28}$$

The asymmetry coefficient is defined as the ratio between the zero and the positive component and is expressed in %. It is calculated using the following expression:

$$\underline{k}^0\% = \frac{\underline{U}^0}{\underline{U}^+} * 100 \tag{29}$$

Considering Equations (3), (7) and (9) for the asymmetry coefficient at the fault location K (110 kV busbars), the next expression is obtained:

$$\underline{k}_K^0 = \frac{\underline{Z}^0}{\underline{Z}^- + \underline{Z}^0 + 3 * R_t} \tag{30}$$

The value of the zero-sequence voltage of the phase voltages related to the medium-voltage busbars (6 kV), and of the low-voltage busbars (0.4 kV) is zero because the HV/MV

transformer has the windings in a triangle connection on the medium-voltage side, and the MV/LV transformer has the medium-voltage windings in a delta connection (Figure 4c).

The values of the phase voltages of the three-phase system of voltages are expressed as a function of the coefficient of dissymmetry and the coefficient of asymmetry through the following relationships:

$$\begin{aligned} \underline{U}_a &= \underline{U}^+\left(1+\underline{k}^- +\underline{k}^0\right) \\ \underline{U}_b &= \underline{U}^+\left(1+\underline{a}^2*\underline{k}^- +\underline{a}*\underline{k}^0\right) \\ \underline{U}_c &= \underline{U}^+\left(1+\underline{a}*\underline{k}^- +\underline{a}^2*\underline{k}^0\right) \end{aligned} \quad (31)$$

During the single-phase-to-ground fault, the phase voltages no longer form a symmetrical three-phase system. As a result, the positive sequence component has a lower value than in the absence of the fault when the three-phase system of phase voltages is symmetrical and contains only the positive sequence component.

The reduction factor of the positive component (k [%]) during the fault compared to the normal operating situation (in the absence of the fault) is determined using the following expression:

$$k[\%] = \frac{U^+}{U_n} * 100 \quad (32)$$

where U^+ represents the positive sequence component of the phase voltages in the presence of the fault, and U_n represents the effective value of the phase voltages in the absence of the fault.

4. Results

Information flow diagram for the numerical calculation of the phase voltages related to the 110 kV, 6 kV and 0.4 kV bars of the transformer station, the dissymmetry and asymmetry coefficients related to the 110 kV, 6 kV and 0.4 kV busbars, and the component reduction coefficient of the plus sequence during the phase earth fault at point K in Figure 1, is shown in Figure 5.

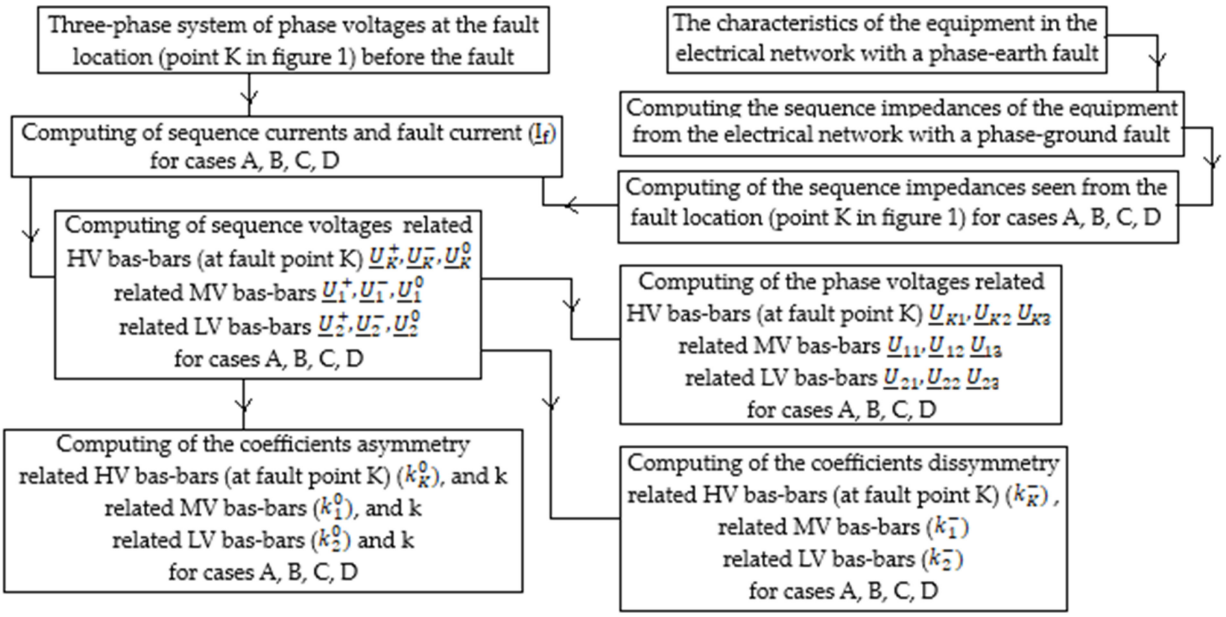

Figure 5. Informational flow diagram for the calculation of phase voltages, and the coefficients of dissymmetry, asymmetry and reduction in the plus sequence.

For the calculation of the fault current, the phase voltages related to the 110 kV, 6 kV and 0.4 kV busbars, the dissymmetry and asymmetry coefficients, and the reduction ratio of the plus sequence component during a single-phase-to-ground fault occurring near the HV busbars of the power station (point K in Figure 1), it is necessary to determine the sequence impedances of the elements that intervene in Figures 1 and 4. The calculation of the sequence impedances requires knowledge of the characteristics of the elements that intervene in Figure 1.

The calculation of the previously specified quantities requires the following steps:

Step 1: Specification of the characteristics of the elements involved in the analysed electrical network;
Step 2: Calculation of the sequence impedances of the elements in Figure 1 and of the impedances that intervene in Figure 3;
Step 3: Implementing the mathematical models presented in Section 2 in the MATCAD programming environment;
Step 4: Performing calculations using the Mathcad (version 13, University of Cambridge, England) programming environment;
Step 5: Presenting the results obtained as complex quantities;
Step 6: Graphical representation of the instantaneous values of the phase voltages related to the 110 kV, 6 kV and 0.4 kV bars.

4.1. Characteristics of the Elements in Figure 1

The characteristics of the elements, respectively the sequence impedances corresponding to them from Figure 1 are presented in Tables 1–6.

Table 1. Characteristics of 110 kV lines.

Line Type		**Simple Circuit**		**Double Circuit**	
L_1	Material	Ol-AL	Ol-AL	Ol-Al	
	Length (km)	22.78	5.16	0.7	
	Section (mm^2)	240	185	240	
L_2	Material	Ol-Al		Ol-Al	Ol-Al
	Length (km)	29.37		14.02	5.08
	Section (mm^2)	185		185	240

Table 2. Sequence impedances of 110 kV lines.

	$\underline{Z}^+$ **[Ω]**	$\underline{Z}^-$ **[Ω]**	$\underline{Z}^0$ **[Ω]**
L_1	4.98 + j9.92	4.98 + j9.92	9.28 + j36.28
L_2	6.49 + j16.31	6.49 + j16.31	15.56 + j69.62

Table 3. Characteristics of transformers.

	U_{1n} **[kV]/** U_{2n} **[kV]**	S_n **[MVA]**	P_{Fe} **[kW]**	P_{Cu} **[kW]**	I_0 **[%]**	U_{sc} **[%]**
Tr.1	110/6	25	30	130	1	11
Tr.3	6/0.4	1.6	2.6	18	2	6

Table 4. Sequence impedances of transformers at voltage level 110 kV.

	$\underline{Z}^{+}$ [Ω]	$\underline{Z}^{-}$ [Ω]	$\underline{Z}^{0}$ [Ω]	
Tr.1	7.55 + j83.24	7.55 + j83.24	The 110 kV winding has the connection Y_0.	The 110 kV winding has the connection Y
			7.55 + j83.24	∞
Tr.3	6.39 + j114.3	6.39 + j114.3	∞	

Table 5. Characteristics of the consumers fed from the 6 kV and 0.4 kV busbars.

	U_n [kV]	P_n [kW]	Number of Motors
Synchronous motors	6	500	21
Asynchronous motors	6	400	4
		160	9
	0.4	160	40

Table 6. Sequence impedances of consumers at the 110 kV voltage level.

	$\underline{Z}^{+}$ [Ω]	$\underline{Z}^{-}$ [Ω]	$\underline{Z}^{0}$ [Ω]
Consumers 6 kV	875.9 + j124.8	875.9 + j31.2	∞
Consumers 0.4 kV	1797 + j256.1	1797 + j84.02	∞

To determine the equivalent sequence impedances of consumers, it was considered that their power factor was 0.93. The resistance value at the fault location (R_t) was 2.8 Ω. The three-phase system of the phase voltages related to the 110 kV busbars, in the absence of the fault, was considered symmetrical and was expressed by the following expressions:

$$\begin{aligned} u_{K1}(t) &= 63.5 * \sqrt{2} * sin(100 * \pi * t)\ \text{kV} \\ u_{K2}(t) &= 63.5 * \sqrt{2} * sin(100 * \pi * t - 120^{\circ})\ \text{kV} \\ u_{K3}(t) &= 63.5 * \sqrt{2} * sin(100 * \pi * t + 120^{\circ})\ \text{kV} \end{aligned} \tag{33}$$

The three-phase voltages are represented in Figure 6.

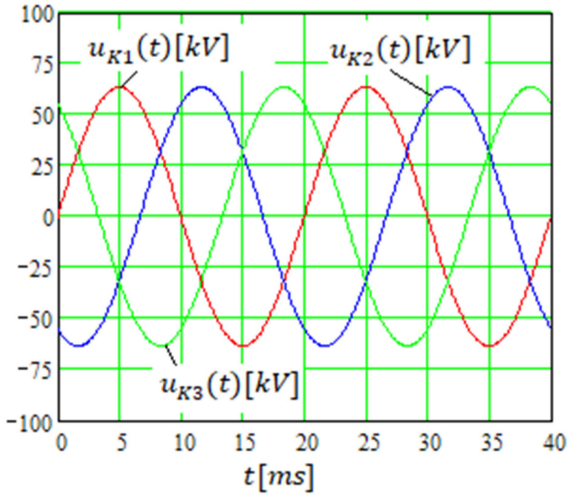

Figure 6. Three-phase system of phase voltages at 110 kV before the fault occurs.

4.2. Computed Results

The numerical results obtained for each of the four cases presented in Section 2 (cases A, B, C and D) are presented below.

Case (A): The 110 kV busbar from the power station is fed by two 110 kV lines (switches S1 and S2 in Figure 1 are connected), the transformer Tr.1 has the connection Y_0/Δ, and the transformer Tr.2 is disconnected from the 110 kV busbar.

The results obtained are shown in Tables 7–9.

Table 7. The values of the current at the fault location ($\underline{I}_f$), of the phase voltages at the fault location ($\underline{U}_{K1}$ $\underline{U}_{K2}$ $\underline{U}_{K3}$), of the sequence voltages at the fault location ($\underline{U}_k^+$, $\underline{U}_k^-$, $\underline{U}_k^0$), of the dissymmetry coefficient (k^-), of the asymmetry coefficient (k^0), and of the plus sequence voltage reduction coefficient (k) in the presence of the single-phase-to-ground fault.

$\mathbf{I_f}$ [kA]	$\underline{\mathbf{U}}_{\mathbf{K1}}$ [kV]	$\underline{\mathbf{U}}_{\mathbf{K2}}$ [kV]	$\underline{\mathbf{U}}_{\mathbf{K3}}$ [kV]	$\underline{\boldsymbol{U}}_{\boldsymbol{k}}^{+}$ [kV]	$\underline{\boldsymbol{U}}_{\boldsymbol{k}}^{-}$ [kV]	$\underline{\boldsymbol{U}}_{\boldsymbol{k}}^{0}$ [kV]	$\boldsymbol{k}^-$ [%]	$\boldsymbol{k}^0$ [%]	**k** [%]
exp(−j59.7°) 5.331 *	exp(−j59.7°) 14.927 *	exp(−j128.7°) 82.895 *	exp(j *138.8°) 68.858 *	exp(−j *1.2°) 51.562 *	exp(−j *174.9°) 12.014	exp(−j *161.5°) 33.798	23.30	65.55	81.19

Table 8. Phase voltages of 6 kV busbars ($\underline{U}_{11}$, $\underline{U}_{12}$, $\underline{U}_{13}$), dissymmetry coefficient (k^-), asymmetry coefficient (k^0) and the plus sequence voltage reduction coefficient (k) in the presence of the single-phase-to-ground fault.

$\underline{\mathbf{U}}_{\mathbf{11}}$ [kV]	$\underline{\mathbf{U}}_{\mathbf{12}}$ [kV]	$\underline{\mathbf{U}}_{\mathbf{13}}$ [kV]	$\underline{\boldsymbol{U}}_{\mathbf{1}}^{+}$ [kV]	$\underline{\boldsymbol{U}}_{\mathbf{1}}^{-}$ [kV]	$\underline{\boldsymbol{U}}_{\mathbf{1}}^{0}$ [kV]	$\boldsymbol{k}^-$ [%]	$\boldsymbol{k}^0$ [%]	**k** [%]
2.065 *exp (−j10.4°)	3.013 *exp (−j117.5°)	3.113 * exp(j101.9°)	2.697 * exp(−j8.6°)	0.636 *exp (−j177.4°)	0	23.58	0	77.86

Table 9. Phase voltages of 0.4 kV busbars ($\underline{U}_{21}$, $\underline{U}_{22}$, $\underline{U}_{23}$), dissymmetry coefficient (k^-), asymmetry coefficient (k^0) and the plus sequence voltage reduction coefficient (k) in the presence of the single-phase-to-ground fault.

$\underline{\mathbf{U}}_{\mathbf{21}}$ [V]	$\underline{\mathbf{U}}_{\mathbf{22}}$ [V]	$\underline{\mathbf{U}}_{\mathbf{23}}$ [V]	$\underline{\boldsymbol{U}}_{\mathbf{2}}^{+}$ [V]	$\underline{\boldsymbol{U}}_{\mathbf{2}}^{-}$ [V]	$\underline{\boldsymbol{U}}_{\mathbf{2}}^{0}$ [V]	$\boldsymbol{k}^-$[%]	$\boldsymbol{k}^0$[%]	**k** [%]
125.1 *exp (−j*13.6°)	182.6 *exp (−j*120.6°)	188.6 * exp(98.7°)	172 *exp (−j *11.7°)	40.6 *exp (−j *174.2°)	0	23.60	0	74.48

The instantaneous values of the phase voltages at the fault location (point K) are given by the following expressions:

$$\begin{aligned} \mathrm{u_{K1}(t)} &= 14.927 * \sqrt{2} * \sin(100 * \pi * \mathrm{t} - 59.7^\circ)\ \mathrm{kV} \\ u_{K2}(t) &= 82.895 * \sqrt{2} * sin(100 * \pi * t - 128.7^\circ)\ \mathrm{kV} \\ \mathrm{u_{K3}(t)} &= 68.858 * \sqrt{2} * \sin(100 * \pi * \mathrm{t} + 138.8^\circ)\ \mathrm{kV} \end{aligned} \tag{34}$$

The instantaneous values of the phase voltages related to the 110 kV busbars are represented in Figure 7.

The instantaneous values of the phase voltages related to the 6 kV busbars in the presence of the single-phase-to-ground fault are given by the following expressions:

$$\begin{aligned} \mathrm{u_{11}(t)} &= 14.927 * \sqrt{2} * \sin(100 * \pi * \mathrm{t} - 59.7^\circ)\ \mathrm{kV} \\ u_{12}(t) &= 82.895 * \sqrt{2} * sin(100 * \pi * t - 128.7^\circ)\ \mathrm{kV} \\ \mathrm{u_{13}(t)} &= 68.858 * \sqrt{2} * \sin(100 * \pi * \mathrm{t} + 138.8^\circ)\ \mathrm{kV} \end{aligned} \tag{35}$$

The instantaneous values of the phase voltages related to the 6 kV bars are represented in Figure 8.

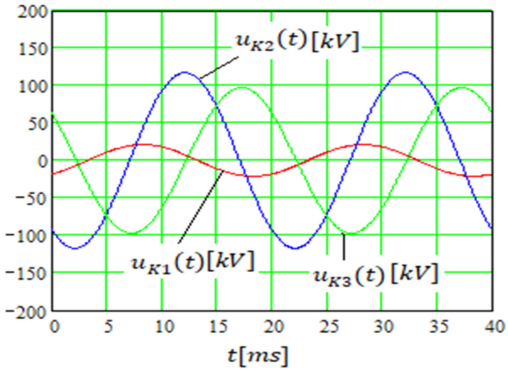

Figure 7. The three-phase system of phase voltages at 110 kV during the fault, case (A).

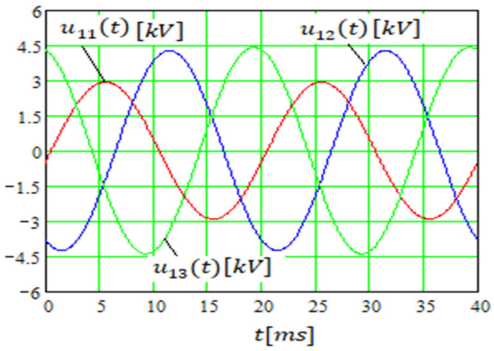

Figure 8. Three-phase system of phase voltages at 6 kV during the fault, case (A).

The instantaneous values of the phase voltages related to the 0.4 kV busbars in the presence of the single-phase fault-to-ground are expressed by the following expressions:

$$\begin{aligned} u_{21}(t) &= 125.1 * \sqrt{2} * \sin(100 * \pi * t - 13.6^\circ)\ V \\ u_{22}(t) &= 182.6 * \sqrt{2} * sin(100 * \pi * t - 120.6^\circ)\ V \\ u_{23}(t) &= 188.6 * \sqrt{2} * \sin(100 * \pi * t + 98.7^\circ)\ V \end{aligned} \quad (36)$$

The instantaneous values of the phase voltages related to the 0.4 kV busbars are represented in Figure 9.

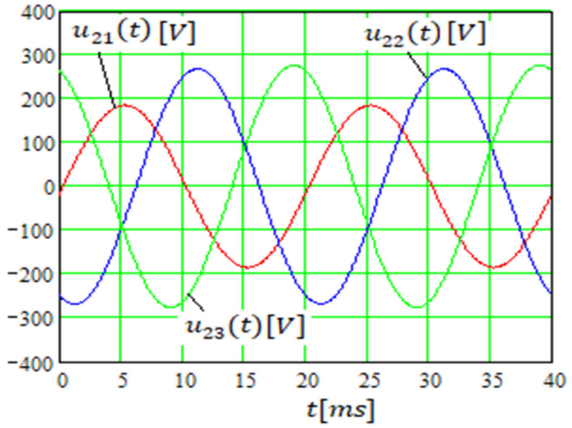

Figure 9. Three-phase system of phase voltages at 0.4 kV during the fault, case (A).

After analysing Equations (34)–(36), it was found that the three-phase system of phase voltages related to the HV busbars was the most non-symmetric. The smallest amplitude was 18% of the largest amplitude of the phase voltages related to the 110 kV busbars, 66.3%

for the voltages related to the 6 kV busbars and 66.8% for the phase voltages related to the 0.4 kV busbars. The difference between the voltages of the phases without a fault was 16.9% for the 110 kV busbars, 3.2% for the 6 kV busbars and 2.91% for the 0.4 kV busbars.

Case (B): The 110 kV busbar from the transformer station are fed by two 110 kV lines (switches S1 and S2 in Figure 1 are connected), transformer Tr.1 has the Y/Δ connection, and transformer Tr.2 is disconnected from the 110 kV busbar.

The results obtained are shown in Tables 10–12.

Table 10. The values of the current at the fault location ($\underline{I}_f$), of the phase voltages at the fault location ($\underline{U}_{K1}$, $\underline{U}_{K2}$, $\underline{U}_{K3}$), of the sequence voltages at the fault location ($\underline{U}_k^+$, $\underline{U}_k^-$, $\underline{U}_k^0$), of the dissymmetry coefficient (k^-), of the asymmetry coefficient (k^0), and of the plus sequence voltage reduction coefficient (k) in the presence of the single-phase-to-ground fault.

$\underline{I}_f$ [kA]	$\underline{U}_{K1}$ [kV]	$\underline{U}_{K2}$ [kV]	$\underline{U}_{K3}$ [kV]	$\underline{U}_k^+$ [kV]	$\underline{U}_k^-$ [kV]	$\underline{U}_k^0$ [kV]	k^- [%]	k^0 [%]	k [%]
4.618 * exp(−j61°)	12.931 * exp(−j61°)	86.473 * exp(−j132°)	73.746 * exp(j141.7°)	53.135 * exp(−j0.7°)	10.408 * exp(−j176.3°)	37.808 * exp(−164.8°)	19.59	71.15	83.67

Table 11. Phase voltages of 6 kV busbars ($\underline{U}_{11}$, $\underline{U}_{12}$, $\underline{U}_{13}$), dissymmetry coefficient (k^-), asymmetry coefficient (k^0) and the plus sequence voltage reduction coefficient (k) in the presence of the single-phase-to-ground fault.

$\underline{U}_{11}$ [kV]	$\underline{U}_{12}$ [kV]	$\underline{U}_{13}$ [kV]	$\underline{U}_1^+$ [kV]	$\underline{U}_1^-$ [kV]	$\underline{U}_1^0$ [kV]	k^- [%]	k^0 [%]	k [%]
2.230 * exp(−j9.2°)	3.060 * exp(−j118.8°)	3.122 * exp(j103.6°)	2.779 * exp(−j8.1°)	0.551 * exp(−j176°)	0	19.83	0	80.22

Table 12. Phase voltages of 0.4 kV busbars ($\underline{U}_{21}$, $\underline{U}_{22}$, $\underline{U}_{23}$), dissymmetry coefficient (k^-), asymmetry coefficient (k^0) and the plus sequence voltage reduction coefficient (k) in the presence of the single-phase-to-ground fault.

$\underline{U}_{21}$ [V]	$\underline{U}_{22}$ [V]	$\underline{U}_{23}$ [V]	$\underline{U}_2^+$ [V]	$\underline{U}_2^-$ [V]	$\underline{U}_2^0$ [V]	k^- [%]	k^0 [%]	k [%]
135.1 * exp(−j12.3°)	185.4 * exp(−j121.9°)	−189.2 * exp(100.3°)	177.3 * exp(−j11.3°)	35.2 * exp(−j172.9°)	0	19.85	0	76.77

The instantaneous values of the phase voltages at the fault location are given by the following expressions:

$$\begin{aligned} u_{K1}(t) &= 12.931 * \sqrt{2} * \sin(100 * \pi * t - 61^\circ) \text{ kV} \\ u_{K2}(t) &= 86.473 * \sqrt{2} * sin(100 * \pi * t - 132^\circ) \text{ kV} \\ u_{K3}(t) &= 73.746 * \sqrt{2} * \sin(100 * \pi * t + 141.7^\circ) \text{ kV} \end{aligned} \quad (37)$$

The instantaneous values of the phase voltages related to the 110 kV busbars are represented in Figure 10.

The instantaneous values of the phase voltages related to the 6 kV busbars in the presence of the single-phase-to-ground fault are given by the following expressions:

$$\begin{aligned} u_{11}(t) &= 2.230 * \sqrt{2} * \sin(100 * \pi * t - 9.2^\circ) \text{ kV} \\ u_{12}(t) &= 3.060 * \sqrt{2} * sin(100 * \pi * t - 118.8^\circ) \text{ kV} \\ u_{13}(t) &= 3.122 * \sqrt{2} * \sin(100 * \pi * t + 103.6^\circ) \text{ kV} \end{aligned} \quad (38)$$

The instantaneous values of the phase voltages related to the 6 kV busbars are represented in Figure 11.

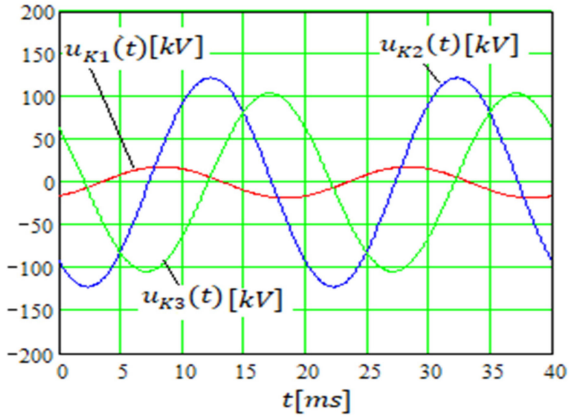

Figure 10. The three-phase system of phase voltages at 110 kV during the fault, case (B).

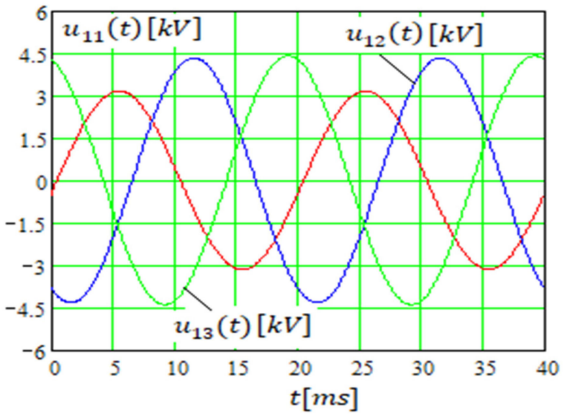

Figure 11. Three-phase system of phase voltages at 6 kV during the fault, case (B).

The instantaneous values of the phase voltages related to the 0.4 kV busbars in the presence of the single-phase-to-ground fault are given by the following expressions:

$$\begin{aligned} u_{21}(t) &= 135.1 * \sqrt{2} * \sin(100 * \pi * t - 12.3^{\circ}) \text{ V} \\ u_{22}(t) &= 185.4 * \sqrt{2} * sin(100 * \pi * t - 121.9^{\circ}) \text{ V} \\ u_{23}(t) &= 189.2 * \sqrt{2} * \sin(100 * \pi * t + 100.3^{\circ}) \text{ V} \end{aligned} \quad (39)$$

The instantaneous values of the phase voltages related to the 0.4 kV busbars are represented in Figure 12.

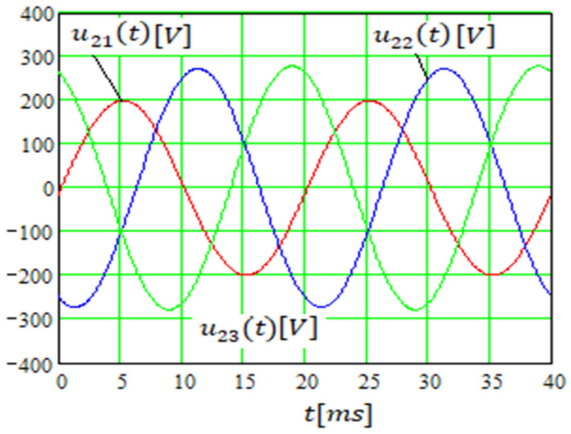

Figure 12. Three-phase system of phase voltages at 0.4 kV during the fault, case (B).

After analysing Equations (37)–(39), it was found that the three-phase system of phase voltages related to the HV busbars was the most non-symmetric. The smallest amplitude was 14.95% of the largest amplitude of the phase voltages related to the 110 kV busbars, 71.66% for the voltages related to the 6 kV busbars and 71.69% for the phase voltages related to the 0.4 kV busbars. The difference between the voltages of the phases without a fault was 14.72% for the 110 kV busbars, 1.67% for the 6 kV busbars and 2.13% for the 0.4 kV busbars.

Case (C): The 110 kV busbar from the transformer station is fed by the 110 kV line L_1 (in Figure 1 the switch S1 is connected and the switch S2 is disconnected), the transformer Tr.1 has the Y_0/Δ connection, and the transformer Tr.2 is disconnected from the 110 kV busbar.

The results obtained are shown in Tables 13–15.

Table 13. The values of the current at the fault location ($\underline{I}_f$), of the phase voltages at the fault location ($\underline{U}_{K1}$, $\underline{U}_{K2}$, $\underline{U}_{K3}$), of the sequence voltages at the fault location ($\underline{U}_k^+$, $\underline{U}_k^-$, $\underline{U}_k^0$), of the dissymmetry coefficient (k^-), of the asymmetry coefficient (k^0), and of the plus sequence voltage reduction coefficient (k) in the presence of the single-phase-to-ground fault.

$\underline{I}_f$ [kA]	$\underline{U}_{K1}$ [kV]	$\underline{U}_{K2}$ [kV]	$\underline{U}_{K3}$ [kV]	$\underline{U}_k^+$ [kV]	$\underline{U}_k^-$ [kV]	$\underline{U}_k^0$ [kV]	k^- [%]	k^0 [%]	k [%]
2.533 * exp(−j68.1°)	7.091 * exp(−j68.1°)	78.922 * exp(−j128.1°)	68.313 * exp(j135.5°)	48.956 * exp(−j0.32°)	14.556 * exp(−j167.3°)	32.554 * exp(−j178.9°)	29.73	66.5	77.09

Table 14. Phase voltages of 6 kV busbars ($\underline{U}_{11}$, $\underline{U}_{12}$, $\underline{U}_{13}$), dissymmetry coefficient (k^-), asymmetry coefficient (k^0) and the plus sequence voltage reduction coefficient (k) in the presence of the single-phase-to-ground fault.

$\underline{U}_{11}$ [kV]	$\underline{U}_{12}$ [kV]	$\underline{U}_{13}$ [kV]	$\underline{U}_1^+$ [kV]	$\underline{U}_1^-$ [kV]	$\underline{U}_1^0$ [kV]	k^- [%]	k^0 [%]	k [%]
1.772 * exp(−j7.5°)	3.008 * exp(−j114.5°)	3.012 * exp(j99.7°)	2.547 * exp(−j7.4°)	0.775 * exp(−j172.7°)	0	30.4	0	73.53

Table 15. Phase voltages of 0.4 kV busbars ($\underline{U}_{21}$, $\underline{U}_{22}$, $\underline{U}_{23}$), dissymmetry coefficient (k^-), asymmetry coefficient (k^0) and the plus sequence voltage reduction coefficient (k) in the presence of the single-phase-to-ground fault.

$\underline{U}_{21}$ [V]	$\underline{U}_{22}$ [V]	$\underline{U}_{23}$ [V]	$\underline{U}_2^+$ [V]	$\underline{U}_2^-$ [V]	$\underline{U}_2^0$ [V]	k^- [%]	k^0 [%]	k [%]
107.4 * exp(−j10.7°)	182.3 * exp(−j117.7°)	182.5 * exp(j96.6°)	162.5 * exp(−j10.6°)	49.4 * exp(−j169.6°)	0	30.4	0	70.36

The instantaneous values of the phase voltages at the fault location are given by the following expressions:

$$\begin{aligned} u_{K1}(t) &= 7.091 * \sqrt{2} * \sin(100 * \pi * t - 68.1^\circ)\ \text{kV} \\ u_{K2}(t) &= 78.922 * \sqrt{2} * sin(100 * \pi * t - 128.1^\circ)\ \text{kV} \\ u_{K3}(t) &= 68.313 * \sqrt{2} * \sin(100 * \pi * t + 135.5^\circ)\ \text{kV} \end{aligned} \quad (40)$$

The instantaneous values of the phase voltages related to the 110 kV busbars are represented in Figure 13.

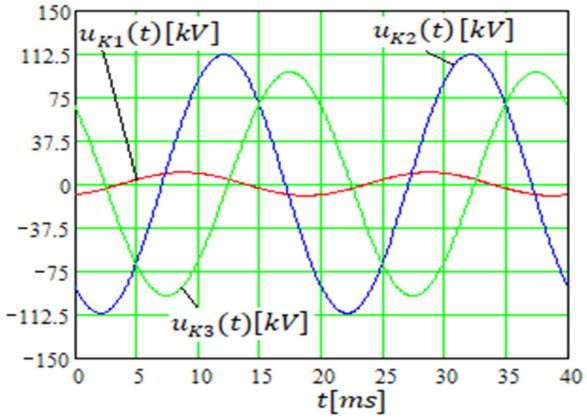

Figure 13. The three-phase system of phase voltages at 110 kV during the fault, case (C).

The instantaneous values of the phase voltages related to the 6 kV busbars in the presence of the single-phase-to-ground fault are given by the next expressions:

$$\begin{aligned} u_{11}(t) &= 1.772 * \sqrt{2} * \sin(100 * \pi * t - 7.5^\circ)\ \text{kV} \\ u_{12}(t) &= 3.008 * \sqrt{2} * sin(100 * \pi * t - 114.5^\circ)\ \text{kV} \\ u_{13}(t) &= 3.012 * \sqrt{2} * \sin(100 * \pi * t + 99.7^\circ)\ \text{kV} \end{aligned} \quad (41)$$

The instantaneous values of the phase voltages related to the 6 kV busbars are represented in Figure 14.

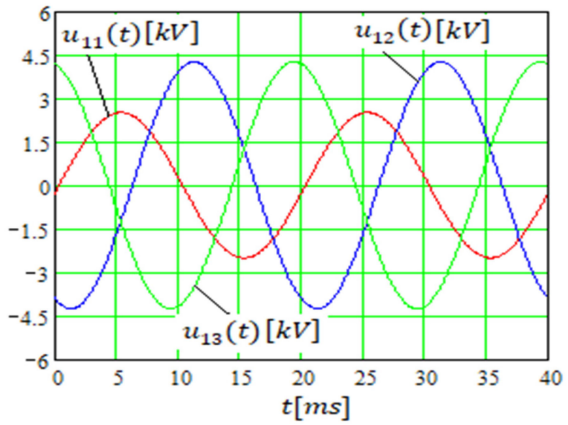

Figure 14. Three-phase system of phase voltages at 6 kV during the fault, case (C).

The instantaneous values of the phase voltages related to the 0.4 kV busbars in the presence of the single-phase-to-ground fault are given by the following expressions:

$$\begin{aligned} u_{21}(t) &= 107.4 * \sqrt{2} * \sin(100 * \pi * t - 10.7^\circ)\ \text{V} \\ u_{22}(t) &= 182.3 * \sqrt{2} * sin(100 * \pi * t - 117.7^\circ)\ \text{V} \\ u_{23}(t) &= 182.5 * \sqrt{2} * \sin(100 * \pi * t + 96.6^\circ)\ \text{V} \end{aligned} \quad (42)$$

The instantaneous values of the phase voltages related to the 0.4 kV busbars are represented in Figure 15.

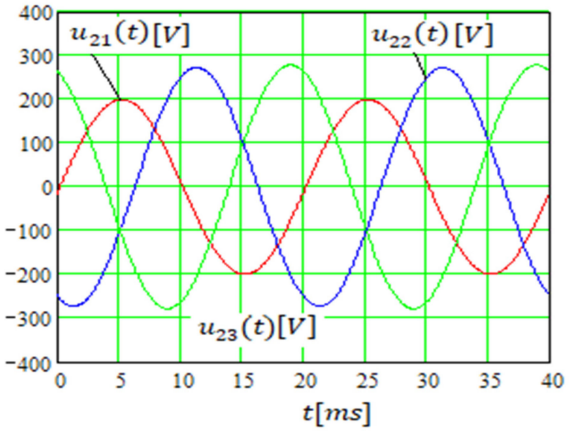

Figure 15. Three-phase system of phase voltages at 0.4 kV during the fault, case (C).

After analysing Equations (40)–(42), it was found that the three-phase system of phase voltages related to the HV busbars was the most non-symmetric. The lowest amplitude was 8.98% of the highest amplitude of the phase voltages related to the 110 kV busbars, 58.83% for the voltages related to the 6 kV busbars and 58.85% for the phase voltages related to the 0.4 kV busbars. The difference between the voltages of the phases without a fault was 13.44% for the 110 kV busbars, 0.13% for the 6 kV busbars and 0.11% for the 0.4 kV busbars.

Case (D): The 110 kV busbar from the power station is fed by the 110 kV line L_1 (in Figure 1 the switch S1 is connected and the switch S2 is disconnected), the transformer Tr.1 has the Y/Δ connection, and the transformer Tr.2 is disconnected from the 110 kV busbar.

The results obtained are shown in Tables 16–18.

Table 16. The values of the current at the fault location ($\underline{I}_f$), of the phase voltages at the fault location ($\underline{U}_{K1}$, $\underline{U}_{K2}$, $\underline{U}_{K3}$), of the sequence voltages at the fault location ($\underline{U}_k^+$, $\underline{U}_k^-$, $\underline{U}_k^0$), of the dissymmetry coefficient (k^-), of the asymmetry coefficient (k^0), and of the plus sequence voltage reduction coefficient (k) in the presence of the single-phase-to-ground fault.

$\underline{I}_f$ [kA]	$\underline{U}_{K1}$ [kV]	$\underline{U}_{K2}$ [kV]	$\underline{U}_{K3}$ [kV]	$\underline{U}_k^+$ [kV]	$\underline{U}_k^-$ [kV]	$\underline{U}_k^0$ [kV]	k^- [%]	k^0 [%]	k [%]
1.764 * exp(−j69.7°)	4.938 * exp(−j69.7°)	87.860 * exp(−j134°)	79.919 * exp(j142.2°)	53.386 * exp(j0.5°)	10.136 * exp(−j177.3°)	41.922 * exp(−j172.3°)	18.99	78.53	84.06

Table 17. Phase voltages of 6 kV busbars ($\underline{U}_{11}$, $\underline{U}_{12}$, $\underline{U}_{13}$), dissymmetry coefficient (k^-), asymmetry coefficient (k^0) and the plus sequence voltage reduction coefficient (k) in the presence of the single-phase-to-ground fault.

$\underline{U}_{11}$ [kV]	$\underline{U}_{12}$ [kV]	$\underline{U}_{13}$ [kV]	$\underline{U}_1^+$ [kV]	$\underline{U}_1^-$ [kV]	$\underline{U}_1^0$ [kV]	k^- [%]	k^0 [%]	k [%]
2.263 * exp(−j6.1°)	3.114 * exp(−j118.7°)	3.068 * exp(j104.2°)	2.792 * exp(−j6.9°)	0.530 * exp(−j169.9°)	0	18.98	0	80.60

Table 18. Phase voltages of 0.4 kV busbars ($\underline{U}_{21}$, $\underline{U}_{22}$, $\underline{U}_{23}$), dissymmetry coefficient (k^-), asymmetry coefficient (k^0) and the plus sequence voltage reduction coefficient (k) in the presence of the single-phase-to-ground fault.

$\underline{U}_{21}$ [V]	$\underline{U}_{22}$ [V]	$\underline{U}_{23}$ [V]	$\underline{U}_2^+$ [V]	$\underline{U}_2^-$ [V]	$\underline{U}_2^0$ [V]	k^- [%]	k^0 [%]	k [%]
137.1 * exp(−j9.3°)	188.7 * exp(−j121.8°)	185.9 * exp(j101.1°)	178.1 * exp(−j10°)	33.8 * exp(−j166.8°)	0	18.98	0	77.12

The instantaneous values of the phase voltages related to the 110 kV busbars in the presence of the single-phase-to-ground fault are given by the next expressions:

$$\begin{aligned} \mathrm{u_{K1}(t)} &= 4.938 * \sqrt{2} * \sin(100 * \pi * \mathrm{t} - 69.7^{\circ}) \text{ kV} \\ u_{K2}(t) &= 87.86 * \sqrt{2} * sin(100 * \pi * t - 134^{\circ}) \text{ kV} \\ \mathrm{u_{K3}(t)} &= 79.919 * \sqrt{2} * \sin(100 * \pi * \mathrm{t} + 142.2^{\circ}) \text{ kV} \end{aligned} \quad (43)$$

The instantaneous values of the phase voltages related to the 110 kV busbars are represented in Figure 16.

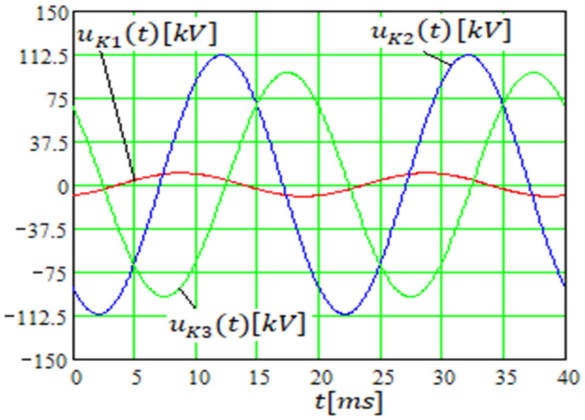

Figure 16. The three-phase system of phase voltages at 110 kV during the fault, case (D).

The instantaneous values of the phase voltages related to the 6 kV busbars in the presence of the single-phase-to-ground fault are given by the next expressions:

$$\begin{aligned} \mathrm{u_{11}(t)} &= 2.263 * \sqrt{2} * \sin(100 * \pi * \mathrm{t} - 6.1^{\circ}) \text{ kV} \\ u_{12}(t) &= 3.114 * \sqrt{2} * sin(100 * \pi * t - 118.7^{\circ}) \text{ kV} \\ \mathrm{u_{13}(t)} &= 3.068 * \sqrt{2} * \sin(100 * \pi * \mathrm{t} + 104.2^{\circ}) \text{ kV} \end{aligned} \quad (44)$$

The instantaneous values of the phase voltages related to the 6 kV busbars are represented in Figure 17.

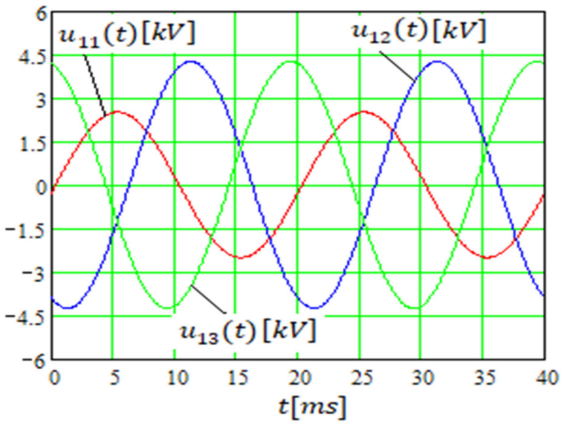

Figure 17. Three-phase system of phase voltages at 6 kV during the fault, case (D).

The instantaneous values of the phase voltages related to the 0.4 kV busbars in the presence of the single-phase-to-ground fault are given by the following expressions:

$$\begin{gathered} u_{21}(t) = 137.1 * \sqrt{2} * \sin(100 * \pi * t - 9.3^\circ)\ V \\ u_{22}(t) = 188.7 * \sqrt{2} * sin(100 * \pi * t - 121.8^\circ)\ V \\ u_{23}(t) = 185.9 * \sqrt{2} * \sin(100 * \pi * t + 101.1^\circ)\ V \end{gathered} \quad (45)$$

The instantaneous values of the phase voltages related to the 0.4 kV busbars are represented in Figure 18.

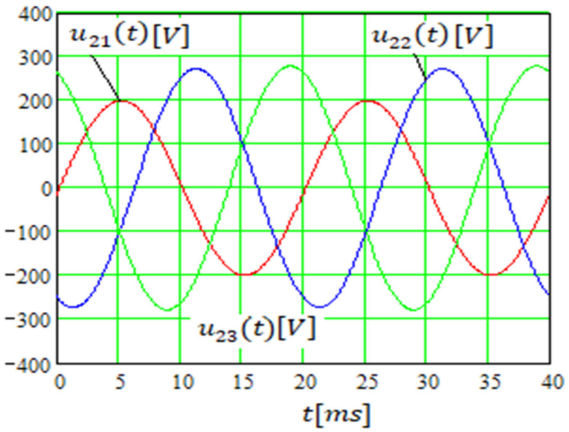

Figure 18. Three-phase system of phase voltages at 0.4 kV during the fault, case (D).

After analysing Equations (43)–(45), it was found that the three-phase system of phase voltages related to the IT busbars was the most non-symmetric. The lowest amplitude was 5.62% of the highest amplitude of the phase voltages related to the 110 kV busbars, 72.67% for the voltages related to the 6 kV busbars and 72.82% for the phase voltages related to the 0.4 kV busbars. The difference between the voltages of the phases without a fault was 10.06% for the 110 kV busbars, 1.48% for the 6 kV busbars and 1.48% for the 0.4 kV busbars.

5. Experimental Determination

A single-phase-to-ground fault on the HV busbars of the power station can have serious consequences for the substation equipment and the consumers fed by it. For this reason, the case in which the value of the fault current was minimal was chosen for the experiment. The 110 kV busbars were fed through the L_2 line, whose impedance was higher than that of the L_1 line (Figure 1). Also, the fault was not caused on the HV busbars of the power station but near them, at approximately 50 m away.

To provoke the single-phase-to-ground fault, phase 1 of the L_1 line was connected to the earthing system of its the first tower.

The earthing resistance of the tower at which the fault was caused was 2.8 Ω (Rt = 2.8 Ω). During the fault, the L_1 line was not fed from the power station (Figure 1). With the help of a control device, designed and made to be used for experimental determinations in real electrical installations, the connection or disconnection command of the switch S_1 related to the L_1 line was ensured (Figure 19). By connecting the switch S_1, the 110 kV busbars of the power station were connected to the single-phase-to-ground fault caused at point K in Figure 19. The experimental determinations were carried out for two cases, namely:

- Case 1: Transformer Tr.1 in Figure 1 had the connection Y_0/Δ (the neutral of the 110 kV transformer winding was grounded).
- Case 2: The transformer Tr 1 in Figure 1 had the Y/Δ connection (the neutral of the 110 kV winding of the transformer was isolated).

The diagram used for the experimental determinations is presented in Figure 19. The phase voltages of the 110 kV busbars and 0.4 kV busbars, and the fault current were

measured. The effective values of the phase voltages and fault current are shown in Tables 19–22.

Table 19. Effective values of phase voltages related to 110 kV busbars (U_{K1}, U_{K2}, U_{K3}) and short-circuit current (I_f).

I_f [A]	U_{K1} [kV]	U_{K2} [kV]	U_{K3} [kV]
2640	7.6	68.7	62.1

Table 20. The effective values of the phase voltages related to the 0.4 kV busbars (U_{21}, U_{22}, U_{23}).

U_{21} [V]	U_{22} [V]	U_{23} [V]
112	206	211

Table 21. Effective values of phase voltages related to 110 kV busbars (U_{K1}, U_{K2}, U_{K3}) and short-circuit current (I_f).

I_f [A]	U_{K1} [kV]	U_{K2} [kV]	U_{K3} [kV]
1830	5.16	79.3	76

Table 22. The effective values of the phase voltages related to the 0.4 kV busbars (U_{21}, U_{22}, U_{23}).

U_{21} [V]	U_{22} [V]	U_{23} [V]
156	214	218

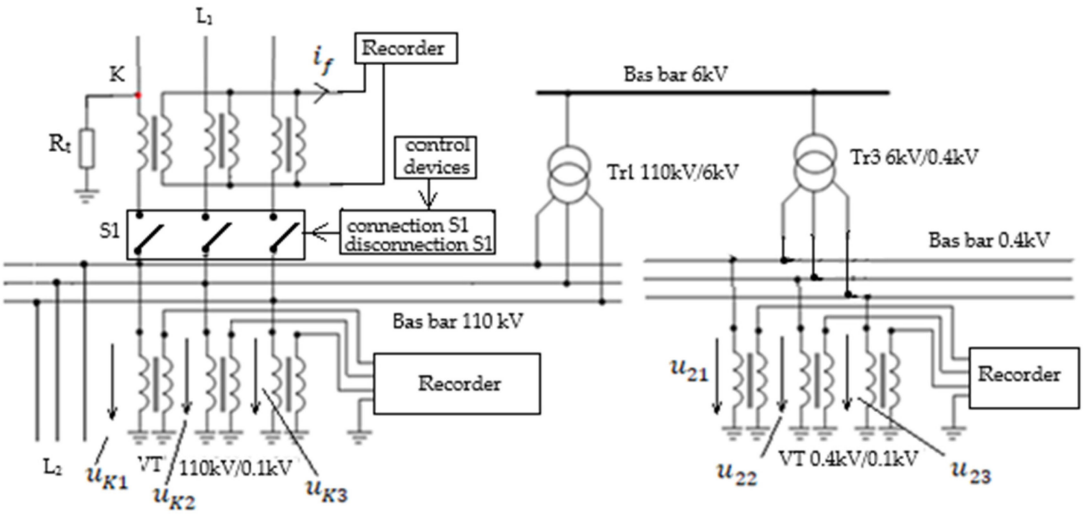

Figure 19. Simplified measurement scheme (The figure was revised).

Case (C): The 110 kV busbar from the power station was fed by the 110 kV line L_1 (in Figure 1 the switch S1 is disconnected and the switch S2 is connected), the transformer Tr.1 had the Y_0/Δ connection, and the transformer Tr.2 was disconnected from the 110 kV busbar.

To provoke the single-phase-to-ground fault, switch S1 was connected. The obtained results are presented in Table 19 for the 110 kV HV busbars and in Table 20 for the 0.4 kV busbars.

Case (D): The 110 kV busbar from the power station was fed by the 110 kV line L_1 (in Figure 1 the switch S1 is disconnected and the switch S2 is connected), the transformer Tr.1 had the Y/Δ connection, and the transformer Tr.2 was disconnected from the 110 kV busbar.

To provoke the single-phase-to-ground fault, switch S1 was connected. The obtained results are presented in Table 21 for the 110 kV IT busbars and in Table 22 for the 0.4 kV busbars.

6. Discussion

6.1. Analysis of the Reduction Coefficient of the Plus Sequence Components during the Single-Phase-to-Ground Fault for the Analysed Cases

Figure 20 presents the reduction factor of the positive component k [%] during the fault compared to the normal operating situation (in the absence of the fault), for each of the four analysed cases (cases A, B, C, D). To calculate this ratio, Equation (32) was used. For the plus sequence component of the phase voltages, the values obtained by calculation were considered for the 110 kV and 0.4 kV busbars.

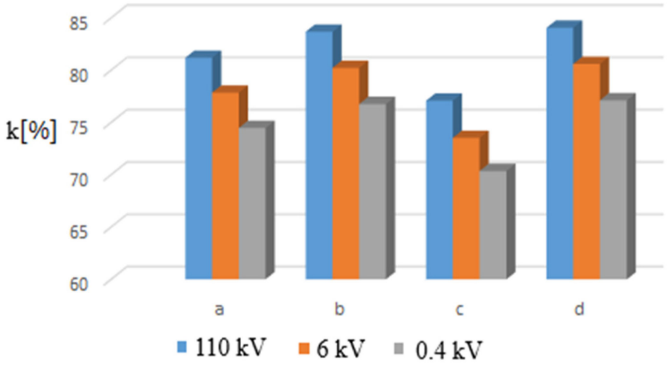

Figure 20. Values of the coefficient k [%] for cases (A)–(D) analysed in the paper.

From Figure 20, it can be seen that when the 110/6 kV transformer had Y/Δ connections during a single-phase-to-ground fault near the 110 kV (HV) busbars, the plus sequence component of the phase voltages decreased the least. As a result, the torque of electric motors fed at 6 kV or 0.4 kV, generated by the plus sequence of the supply voltages during the single-phase-to-ground fault, decreased the least. Consequently, the use of HV/MV transformers with a Y/Δ connection is the most advantageous.

6.2. Comparison between Coefficients of Dissymmetry

Figure 21 shows the values of the k^-% dissymmetry coefficient (the ratio between the negative sequence component and the positive sequence component) related to the busbar phase voltages of 110 kV, 6 kV and 0.4 kV, considering the four analysed cases (cases (A)–(D)). The Equations (26)–(28) were used to calculate the dissymmetry coefficients.

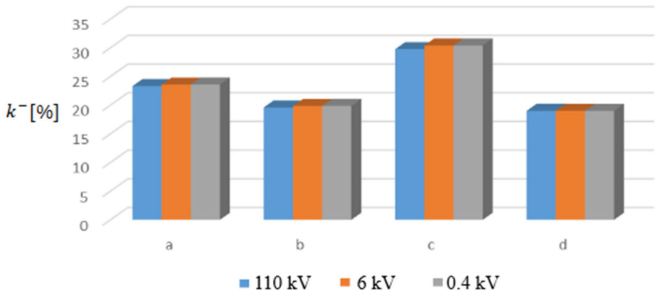

Figure 21. Values of the coefficient k^- [%] for cases (A)–(D) analysed in the paper.

From Figure 19, it can be seen that when the 110/6 kV transformer had the Y/Δ connections, during a single-phase-ground fault near the 110 kV (HV) busbars, the minus sequence component of the phase voltages related to the 110 kV, 6 kV and 4 kV busbars had a lower value than if the 110/6 kV transformer had Y_0/Δ connections. As a result,

the torque of electric motors fed at 6 kV or 0.4 kV generated by the minus sequence of the supply voltages during the single-phase-to-ground fault was less than if the 110/6 kV transformer had a Y_0/Δ connection.

6.3. Comparison of Asymmetry Coefficients

Figure 22 shows the asymmetry coefficient $k^0\%$ (the ratio between the negative sequence component and the positive sequence component) related to the busbar voltages of 110 kV, 6 kV and 0.4 kV, considering the four cases (A)–(D) analysed in this study. Equation (30) was used to calculate the asymmetry coefficients.

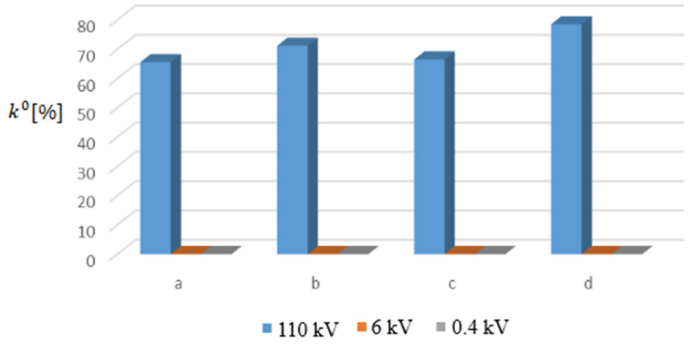

Figure 22. Values of the coefficient k^0 [%] for cases (A)–(D) analysed in the paper.

Figure 22 shows that the zero-sequence component was zero on the 6 kV and 0.4 kV busbars in all four cases analysed. This is because the 110/6 kV transformer had the Y_0/Δ or Y/Δ connection and the 6/0.4 kV transformer had a Δ/Y_0 connection. If the 110 kV busbars were fed by a single transmission line (the source impedance is maximum) and the neutral of the 110 kV/6 kV transformer was isolated, the zero-sequence component of the phase voltages of the 110 kV busbars during the fault would have the largest values.

6.4. Comparison between the Effective Values of the Phase Voltages Determined Experimentally, by Calculation

For the difference, expressed in %, between the values of the fault current and of the phase voltages, obtained by calculation and determined experimentally, the following relationship was used:

$$\varepsilon\% = \frac{\text{Calculated size} - \text{Measured size}}{\text{Measured size}} * 100, \quad (46)$$

The results obtained are presented in Tables 23 and 24.

Table 23. The effective values of the fault current obtained by calculation and experimentally, and the difference between the two values expressed in % (Equation (46)).

	$\mathbf{I_f}$ **[A]**		ε%
	Computed	**Measured**	
Case (C)	2866	2640	7.89
Case (D)	1867	1830	1.98

Table 24. The effective values of the phase voltages (denoted by U_1, U_2, U_3) of the 110 kV and 0.4 kV busbars, obtained by calculation and experimentally, and the difference between these values expressed in % (Equation (46)).

	U_n [kV]	U_1 [V]			U_2 [V]			U_3 [V]		
		Computed	Measured	ε%	Computed	Measured	ε%	Computed	Measured	ε%
Case (C)	110	8025	7600	5.296	74,439	68,700	7.71	65,045	62,100	4.53
	0.4	121.86	112	8.091	225.17	206	8.514	230.13	211	8.313
Case (C)	110	5227	5160	1.28	86,144	79,300	7.945	78,767	76,000	3.513
	0.4	167.51	156	6.871	235.02	214	8.944	234.52	218	7.044

Figures 23–26 show the actual values of the phase voltages of the 110 kV and 0.4 kV busbars, obtained using established mathematical models and by measurements at the actual transformer station.

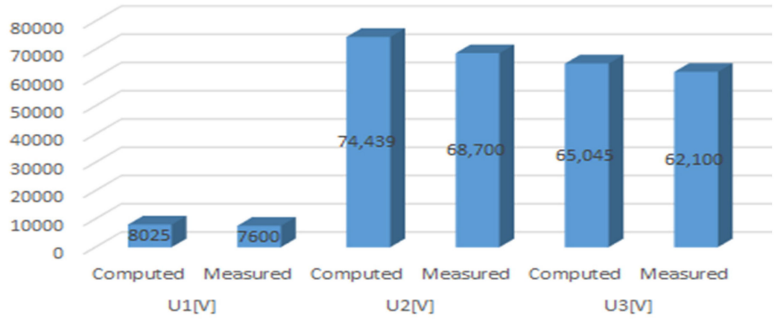

Figure 23. The effective value of the phase voltages of the 110 kV busbars, calculated and measured, for case (C).

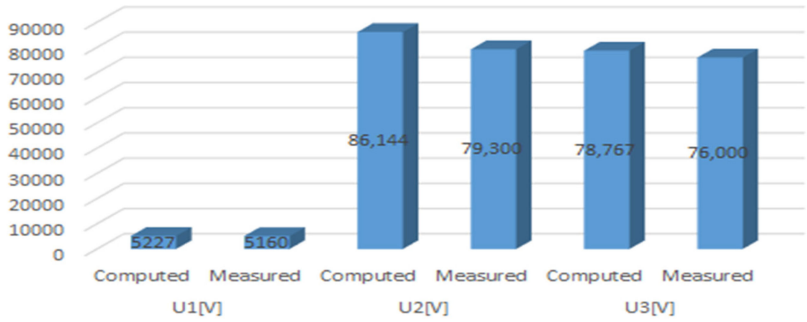

Figure 24. The effective value of the phase voltages of the 110 kV busbars, calculated and measured, for case (D).

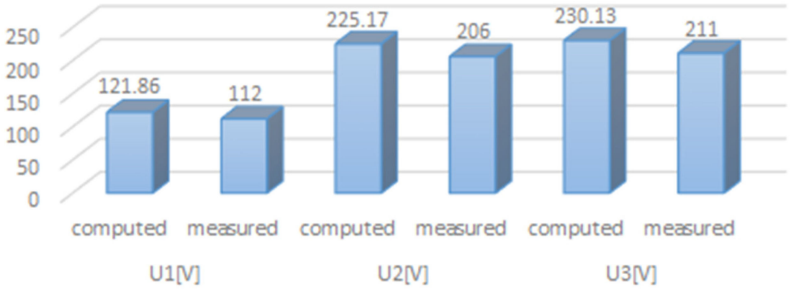

Figure 25. The effective value of the phase voltages of the 0.4 kV busbars, calculated and measured, for case (C).

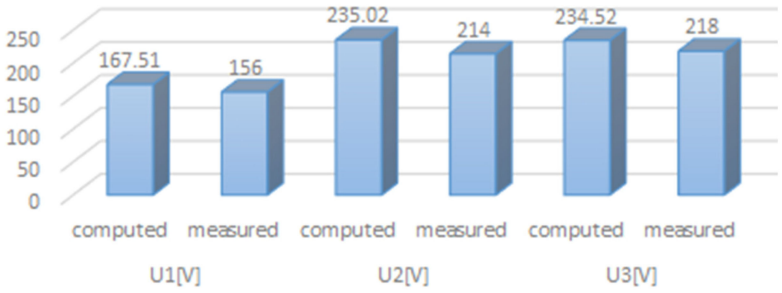

Figure 26. The effective value of the phase voltages of the 0.4 kV busbars, calculated and measured, for case (D).

Figures 27 and 28 present the calculation error of the actual values of the phase voltages of the 110 kV busbars, i.e., 0.4 kV, expressed as a percentage (Equation (46)), for cases (C) and (D).

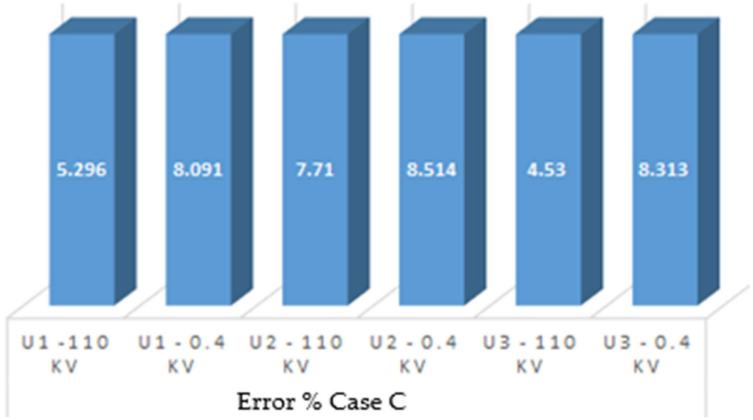

Figure 27. The calculation error of the actual values of the phase voltages of the 110 kV busbars, i.e., 0.4 kV, expressed as a percentage (Equation (46)), for case (C).

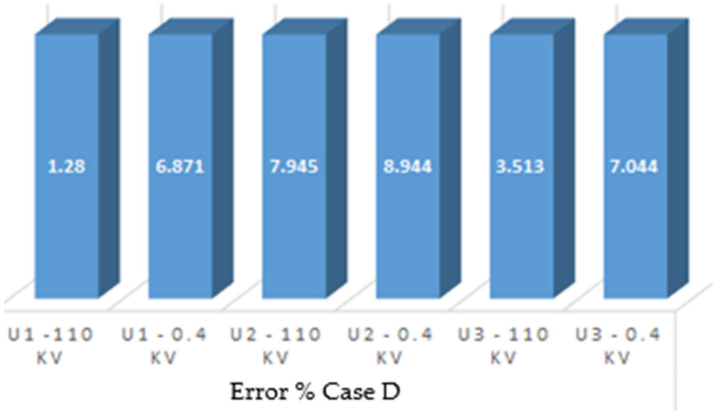

Figure 28. The calculation error of the actual values of the phase voltages of the 110 kV busbars, i.e., 0.4 kV, expressed as a percentage (Equation (46)), for case (D).

Comparing the effective values of the phase voltages obtained by calculation using the mathematical models of Section 3, Equations (16)–(18) for the phase voltages of the 110 kV busbars and Equations (22)–(24) for the 0.4 kV busbars with those determined experimentally in the real installation (Figure 19), it was found that the difference between them was acceptable. From the diagrams presented in Figures 27 and 28, it can be seen that the calculation error (considering the correct values of the quantities obtained from the measurements made in the real installation) of the phase voltages related to the 110 kV

bars, using the mathematical models established in this paper, were between 1.28% and 7.945%. Moreover, for the phase voltages related to the 0.4 kV bars, the calculation errors were between 6.871% and 8.944%. Considering the precision with which the values of the parameters involved in the mathematical models of the phase voltages are known, we considered that the mathematical models established in the paper were correct.

6.5. Comparison between the Effective Values of the Phase Voltages during the Single-Phase-to-Ground Fault and the Values in Normal Operating Mode

To compare the effective values of the phase voltages related to the 110 kV, 6 kV and 0.4 kV busbars during the single-phase-ground fault with those in the normal operating mode (in the absence of the fault), the coefficient k_p% was defined through the following relationship:

$$k_p\% = \frac{U_{kf}}{U_{kn}} * 100 \quad (47)$$

where k represents the number of the phase, i.e., $k \in \{1, 2, 3\}$; U_{kf} represents the effective values of the phase voltages during the fault; and U_{kn} represents the effective values of the phase voltages in normal operation mode (in the absence of the fault).

The results obtained are presented in Table 25. Figure 27 shows the values of the coefficient k_p% for the faulted phase, and Figures 29–31 show the values of the coefficient k_p% for the phases without a fault.

Table 25. Values of the coefficient k_p% for the four cases analysed in the paper.

	The Line Voltages of the Busbars in the Absence of the Fault [kV]	Case (A)	Case (B)	Case (C)	Case (D)
Phase 1 (with fault)	110	25.16	15.22	12.64	8.23
	6	59.76	48.58	47.92	65.88
	0.4	65.82	53.47	52.77	72.53
Phase 2 (without fault)	110	126.5	120.7	117.2	135.6
	6	88.94	90.33	88.65	92.49
	0.4	95.31	99.34	97.5	101.8
Phase 3 (without fault)	110	104.4	96.51	102.4	124
	6	93.44	88.8	90.27	92.06
	0.4	104.4	98.03	99.65	101.6

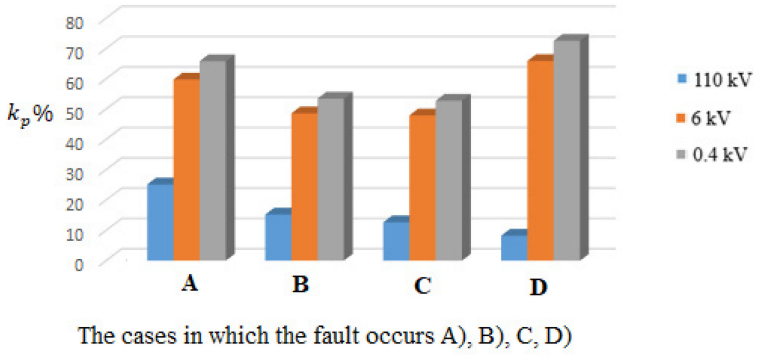

Figure 29. Values of the coefficient k_p [%] for the faulted phase (phase 1) during the fault on phase 1.

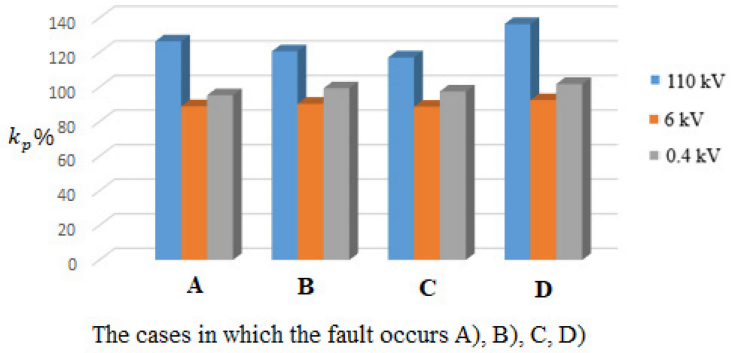

Figure 30. Values of the coefficient k_p [%] for phase 2 (phase without fault) during the fault on phase 1.

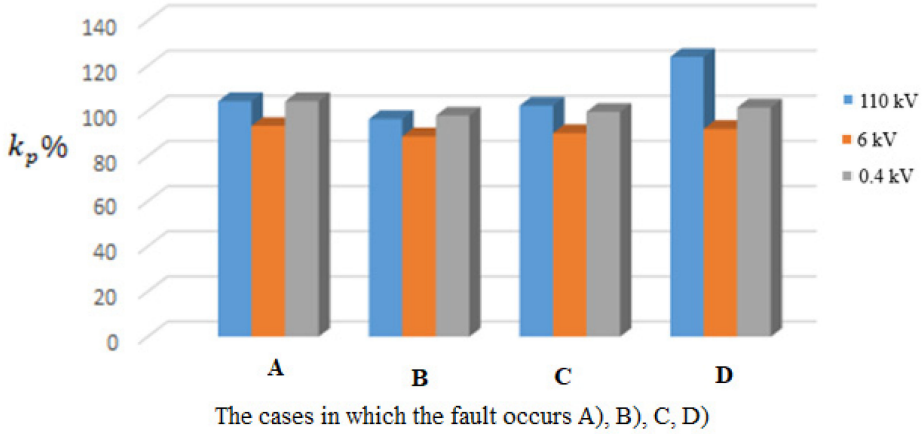

Figure 31. Values of the coefficient k_p [%] for phase 3 (phase without fault) during the fault on phase 1.

After analysing Figures 29–31, it was found that, during a single-phase-to-ground fault, the effective values of the phase voltages changed the most when the two 110 kV lines were connected to the 110 kV busbars of the substation and the neutral of the transformer 110/6 kV was grounded (HV/MV transformer has Y_0/Δ connection). The same was true when the 110 kV L_1 line was connected to the 110 kV busbars of the power station and the neutral of the 110/6 kV transformer had a Y_0/Δ connection. Also, the change in the phase voltages related to the MV (6 kV) and LV (0.4 kV) busbars during the single-phase-to-ground fault was much lower than for the HV (110 kV) busbars. This situation is justified by the fact that the phase voltages of the HV busbars also contain the zero-sequence component, and those related to the MV and LV busbars do not contain the zero-sequence component.

7. Conclusions

Due to the serious consequences of electrical short-circuits on electrical installations, obtaining experimental results to validate the mathematical models used is often a challenge for researchers in this field. Therefore, making experimental results available to the academic community is always useful and welcome.

The most important conclusions resulting from the study are the following:

1. A fault of the single-phase-to-ground type that occurs on the 110 kV lines near the 110 kV busbars, through which the 110/6/0.4 kV power station is supplied, leads to a change in the effective values of the related phase of the HV, MV and LV busbars (Tables 7–18), which affects the operation of the consumers fed from the MV and LV busbars.
2. The degree of change in the phase voltages is influenced by the value of the source impedance (the length of the HV lines that feed the HV busbars in the power station)

at all three voltage levels HV (110 kV), MV (6 kV) and LV (0.4 kV). The higher the source impedance, the lower the reduction in phase voltages (Figures 29–31).

3. An important role in determining the value of the dissymmetry and asymmetry coefficients is played by the neutral point configuration of the HV/MV transformer. If the neutral point of the transformer is connected directly to the ground (the HV/MV transformer has a Y_0/Δ connection), the values of the dissymmetry coefficient are higher than if the neutral point of the HV transformer is isolated (the HV/MV transformer has a Y/Δ connection), Figure 21.
4. Since the MV windings of the HV/MV and MV/LV transformers have a Δ connection, the zero-sequence component of the phase voltages related to the MV and LV busbars is zero. As a result, the asymmetry coefficient of the phase voltages related to the MV and LV busbars has zero value (Figure 22).
5. To reduce the asymmetry of the phase voltages related to the medium-voltage and low-voltage busbars, it is necessary that the neutral point of the HV/MV transformer is isolated. This means that the HV/MV transformer must have Y/Δ connections.
6. The comparison of the effective values of the phase voltages of the high- and low-voltage busbars obtained computationally, using the mathematical models presented in Section 3, with those determined experimentally, and presented in Section 5, validates the mathematical models. The biggest difference between the values determined by calculation was 8.944% (Table 24 and Figure 28).
7. The analytical models for the calculation of the sequence voltages, the dissymmetry coefficients, the asymmetry coefficients and the phase voltages related to the HV, MV and LV busbars presented in this paper can be implemented in a programming environment, for example MATCAD. This represents a very effective tool for the analysis of a phase-to-ground fault.
8. The mathematical models presented in the paper can be used for the analysis of earth phase faults and for other power stations. This would require a different value of the sequence impedances involved in the mathematical models.

Author Contributions: Conceptualization, D.T. and M.V.; methodology, D.T.; software, D.T. and M.V.; validation, D.T.; formal analysis, M.V.; investigation, D.T.; resources, D.T.; data curation, M.V.; writing—original draft preparation, D.T.; writing—review and editing, M.V.; supervision, D.T.; project administration, D.T. All authors have read and agreed to the published version of the manuscript.

Funding: This research received no external funding.

Data Availability Statement: The data presented in the paper, obtained by calculation and experimentally, have not published. Consequently, data sharing is not applicable to this article.

Conflicts of Interest: The authors declare no conflict of interest.

References

1. Perez-Arriaga, I.J.; Rudnick, H.; Abbad, M.R. Electric Energy Systems: An Overview. In *Electric Energy Systems, Analysis and Operation*, 2nd ed.; CRC Press Taylor & Francis Group: Boca Raton, FL, USA; London, UK; New York, NY, USA, 2018.
2. El-Hawary, M. *Electric Energy Systems*, 2nd ed.; CRC Press Taylor & Francis Group: Boca Raton, FL, USA, 2018.
3. Blume, S.W. *Electric Energy System Basics for the Nonelectrical Professional*, 2nd ed.; John Wiely & Sons, Inc.: Hoboken, NJ, USA, 2007.
4. NP-099-04 Normativ Pentru Proiectarea, Executarea, Verificarea Si Exploatarea Instalatiilor Electrice in Zone Cu Pericol de Explozie | PDF (scribd.com) NP-099-04 Regulations for the Design, Execution, Verification and Operation of Electrical Installations in Areas with Danger of Explosion. Available online: https://www.scribd.com/doc/310499498/NP-099-04-Normativ-Instalatii-Electrice-in-Mediul-Exploziv# (accessed on 23 March 2023).
5. Tarko, R.; Gajdzica, J.; Nowak, W.; Szpyra, W. Comparative Analysis of High-Voltage Power Line Models for Determining Short-Circuit Currents in Towers Earthing Systems. *Energies* **2021**, *14*, 4729. [CrossRef]
6. Toader, D.; Greconici, M.; Vesa, D.; Vintan, M.; Solea, C. Analysis of the Influence of the Insulation Parameters of Medium Voltage Electrical Networks and of the Petersen Coil on the Single-Phase-to-Ground Fault Current. *Energies* **2021**, *14*, 1330. [CrossRef]
7. Rashevskaya, M.; Lipinskiy, G.; Tsyruk, S. Applicability of Calculation Methods for Single-phase Short Circuit în Grid with Voltage up to 1 kV. In Proceedings of the 21-st International Symposium on Electrical Apparatus & Technologies, Burgas, Bulgaria, 3–6 June 2020.

8. German, L.A.; Serebryakov, A.S.; Osokin, V.L.; Subkhanverdiev, K.S. Equivalent Scheme for Calculating Short-Circuit Current in an Alternating-Current Electric Traction Network. *Russ. Electr. Eng.* **2019**, *90*, 516–521. [CrossRef]
9. Li, Y.; Zhang, H.; Xu, J. Analysis of Single-phase Short-circuit Current Suppression Measures at Converter Stations and Their Effects on Power System Reliability. In Proceedings of the IEEE Asia Power and Energy Engineering Conference (APEEC), Chengdu, China, 29–31 March 2019.
10. Jian, Y.; Shurui, M.; Xiaodong, L.; Zheng, X. Influence Mechanism and Suppression Control of the MMC on Short-Circuit Current Under AC Faults. *IEEE Access* **2020**, *8*, 138307–138317.
11. Hong, H.; Yu, M.; Zhang, X.; Huan, J.; Sui, Y.; Pan, X. Practical Calculation Method for the Short-Circuit Current of Power Grids with High Temperature Superconducting Fault Current Limiters. *J. Electr. Eng. Technol.* **2020**, *15*, 945–953. [CrossRef]
12. Rustemlı, S.; Demir, İ. Analysis and simulation of single phase-to-ground short circuit fault in Van 154 kV substation: An experimental assessment. *Bitlis Eren Univ. J. Sci. Technol.* **2019**, *9*, 76–82. [CrossRef]
13. Wang, X.; Li, Y.; Zhang, H.; Sun, X.; Lun, T. The Study of Mechanism and Limit Measures for 500kV Single Phase Short Circuit Current Exceeding Limit in UHVDC Converter Station. In Proceedings of the IEEE Innovative Smart Grid Technologies—Asia (ISGT Asia), Chengdu, China, 21–24 May 2019.
14. Castro, L.M.; Guillen, D.; Trillaud, F. On Short-Circuit Current Calculations Including Superconducting Fault Current Limiters (ScFCLs). *IEEE Trans. Power Deliv.* **2018**, *33*, 2513–2523. [CrossRef]
15. Panova, E.A.; Sabirova, R.R.; Novikov, I.V. Specified Model of a Double-Circuit Transmission Line with Two Ground Wires for Calculating a Single-Phase Short Circuit Current in a Network with an Effectively Grounded Neutral. In Proceedings of the International Russian Automation Conference (RusAutoCon), Sochi, Russia, 4–10 September 2022.
16. Available online: https://cauk.tv/articles/power-quality-issues-voltage-and-phase-balancing/ (accessed on 27 March 2023).
17. Chan, J.Y.; Milanovic, J.V.; Delahunty, A. Risk-based assessment of financial losses due to voltage sag. *IEEE Trans. Power Del.* **2011**, *26*, 492–500. [CrossRef]
18. Djokic, S.Z.; Desmet, J.; Vanalme, G.; Milanovic, J.V.; Stockman, K. Sensitivity of personal computers to voltage sags and short interruptions. *IEEE Trans. Power Del.* **2005**, *20*, 375–383. [CrossRef]
19. Djokic, S.Z.; Stockman, K.; Milanovic, J.V.; Desmet, J.J.M.; Belmans, R. Sensitivity of AC adjustable speed drives to voltage sags and short interruptions. *IEEE Trans. Power Del.* **2005**, *20*, 494–505.
20. IEEE Std 1346-1998 IEEE Recommended Practice for Evaluating Electric Power System Compatibility Wit. Available online: https://pdfcoffee.com/ieee-1346-1998-4-pdf-free.html (accessed on 12 March 2023).
21. Overview of IEEE STD 1564-2014 Guide for Voltage Sag Indices. Available online: https://powerquality.blog/2021/03/12/overview-of-ieee-std-1564-2014-guide-for-voltage-sag-indices/ (accessed on 12 March 2023).
22. Park, C.H.; Hong, J.H.; Jang, G. Assessment of system voltage sag performance based on the concept of area of severity. *IET Gen. Transm. Distrib.* **2010**, *4*, 683–693. [CrossRef]
23. Lu, C.N.; Shen, C.C. A voltage sag index considering compatibility between equipment and supply. *IEEE Trans. Power Del.* **2007**, *22*, 996–1002.
24. Tan, R.H.G.; Ramachandaramurthy, V.K. Voltage sag acceptability assessment using multiple magnitude-duration function. *IEEE Trans. Power Del.* **2012**, *27*, 1984–1990. [CrossRef]
25. Tleis, N.D. *Power Systems Modelling and Fault Analysis: Theory and Practice*; Newnes (imprint of the Elsevier): Oxford, UK; Burlington, MA, USA,, 2008.
26. Rui, L.; Nan, P.; Zhi, Y.; Zare, F. A novel single-phase-to-earth fault location method for distribution network based on zero-sequence components distribution characteristics. *Int. J. Electr. Power Energy Syst.* **2018**, *102*, 11–22. [CrossRef]
27. Paul, D. Phase-Ground Fault Current Analysis and Protection of a High-Resistance Grounded Power System. *IEEE Trans. Ind. Appl.* **2020**, *56*, 3306–3314. [CrossRef]
28. Olejnik, B. Alternative method of determining zero-sequence voltage for fault current passage indicators in overhead medium voltage networks. *Electr. Power Syst. Res.* **2021**, *201*, 107506. [CrossRef]

Disclaimer/Publisher's Note: The statements, opinions and data contained in all publications are solely those of the individual author(s) and contributor(s) and not of MDPI and/or the editor(s). MDPI and/or the editor(s) disclaim responsibility for any injury to people or property resulting from any ideas, methods, instructions or products referred to in the content.